ACS OMEGA

Open Access

http://pubs.acs.org/journal/acsodf

Article

Novel Chitosan-Coated Liposomes Coloaded with Exemestane and Genistein for an Effective Breast Cancer Therapy

Shwetakshi Sharma, Priya Gupta, S. M. Kawish, Shahnawaz Ahmad, Zeenat Iqbal, Divya Vohora,* and Kanchan Kohli*

Cite This: *ACS Omega* 2024, 9, 9735−9752

Read Online

ACCESS | Metrics & More | Article Recommendations | Supporting Information

ABSTRACT: For achieving high effectiveness in the management of breast cancer, coadministration of drugs has attracted a lot of interest as a mode of therapy when compared to a single chemotherapeutic agent that often results in reduced therapeutic end results. Owing to their proven effectiveness, good patient compliance, and lower costs, oral anticancer drugs have received much attention. In the present work, we formulated the chitosan-coated nanoliposomes loaded with two lipophilic agents, namely, exemestane (EXE) and genistein (GEN). The formulation was prepared using the ethanol injection method, which is considered a simple method for getting the nanoliposomes. The formulation was optimized using Box−Behnken design (BBD) and was extensively characterized for particle size, ζ-potential, Fourier transform infrared (FTIR), differential scanning calorimetry (DSC), and X-ray diffraction (XRD) analysis. The sizes of conventional and coated liposomes were found to be 104.6 ± 3.8 and 120.3 ± 6.4 nm with a low polydispersity index of 0.399 and 0.381, respectively. The ζ-potential of the liposomes was observed to be −16.56 mV, which changed to a positive value of +22.4 mV, clearly indicating the complete coating of the nanoliposomes by the chitosan. The average encapsulation efficiency was found to be between 70 and 80% for all prepared formulations. The compatibility of the drug with excipients and complete dispersion of the drug inside the system were verified by FTIR, XRD, and DSC studies. Furthermore, the *in vitro* release studies concluded the sustained release pattern following the Korsmeyer-Peppas model as the best-fitting model with Fickian diffusion. *Ex vivo* studies showed better permeation of the chitosan-coated liposomes, which was further confirmed by confocal studies. The prepared chitosan-coated liposomes showed superior antioxidant activity (94.56%) and enhanced % cytotoxicity (IC50 7.253 ± 0.34 μM) compared to the uncoated liposomes. 3-(4,5-Dimethylthiazol-2-yl)-2,5-diphenyltetrazolium bromide (MTT) assay displayed better cytotoxicity of the chitosan-coated nanoliposomes compared to the plain drug, showing the better penetration and enhanced bioavailability of drugs inside the cells. The formulation was found to be safe for administration, which was confirmed using the toxicity studies performed on an animal model. The above data suggested that poorly soluble lipophilic drugs could be successfully delivered via chitosan-coated liposomes for their effective delivery in breast cancer.

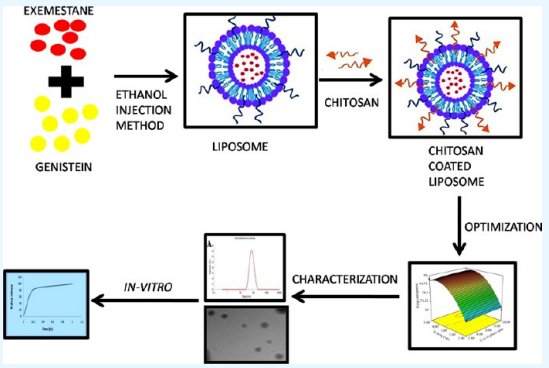

1. INTRODUCTION

Among the most common form of cancer diagnosed in the female population throughout the world, breast cancer has been ranked to be at the first place.[1] The severity of this disease could be judged from the fact that it has replaced lung cancer as the most deadly form of cancer globally. The latest statistics has shown that there will be 1 case of breast cancer out of every 8 cases of cancer diagnosed globally.[2] Its severity can be judged from the fact that in 2020 alone approximately 685,000 women lost their lives due to breast cancer, which rang an alarm bell throughout the scientific communities across the globe and led to the beginning of the World Health Organization (WHO)-led initiative called "Global Breast Cancer Initiative".[3] Under this initiative, efforts were made to bring together various global agencies under one umbrella so that an effective strategy could be planned for early diagnosis, proper treatment, and efficient patient management. Some of the conventional forms of therapy for combating breast cancer are chemotherapy along with surgery and radiation-based therapy.[4] Although these are standard methods and have been used for decades for breast cancer treatment, and in many cases some level of success has been achieved, none of these approaches have fully controlled the progress of this deadly disease. In the majority of the cases, resistance to therapy and relapse of the disease have been observed, creating

Received: December 13, 2023
Revised: January 18, 2024
Accepted: January 30, 2024
Published: February 16, 2024

the need for some alternate therapy that could provide relief to the suffering population. Cancer cells often utilize various complex pathways and mechanisms to propagate and escape the action of therapeutic drugs. In this regard, the action of single-drug therapy often triggers the development of alternative pathways leading to chemotherapeutics resistance mutation and relapse. The application of combination therapy has been proven to be a handy tool in this context. In this approach, often two drugs are used in combination so that they act through different mechanisms, thus causing a synergistic action that deters the emergence of drug resistance.[5]

Exemestane (EXE) is a well-known and approved chemotherapeutic moiety commonly known as an aromatase inactivator (AI), which performs its action by irreversibly binding to the aromatase enzymes responsible for the synthesis of estrogen. This binding caused a gradual decrease in the level of estrogen, thus reducing the aggressive growth of cancer. Exemestane is the third-generation first-line therapy for cases of (hormone-dependent) breast cancer in womenfolk, given via the oral route. Despite its potent antitumor efficacy, its application is usually restricted due to its poor aqueous solubility and compromised oral bioavailability.[6] Patients treated with EXE may suffer from osteoporosis and bone fracture due to the bone loss caused as a side effect.

On the other hand, genistein (GEN), the most abundant isoflavone component extracted from soyabean, has been reported to be an antioxidant and antineoplastic agent. Various available studies have reported its potential in inhibiting cancer cell growth improvement in the health of bones.[7−11] Due to its close structural closeness to the estrogen, it usually competes with the estrogen at the receptor binding site, thus causing a hurdle to the binding of estrogen at the binding pocket; additionally, it also causes metabolism of estrogen, creating an overall favorable condition that suppresses the tumor growth.[12] It also performs its anticancer effect by inhibiting the protein-tyrosine kinase (PTK)-dependent signaling pathway, which leads to the arrest of cancer cells.[13] It has also been utilized as an individual or in combination in various formulations along with chemotherapeutic agents to solve the problem of drug resistance and drug efflux. Asiatic women with a high intake of soy products that constitute isoflavones have shown declined risks of cardiovascular disease, breast cancer, uterine cancer, and osteoporosis. Considering the promising benefits of GEN, it was ideal to combine it with EXE to attain advanced therapeutic efficiency with fewer side effects. This novel combination prevents bone hunting, one of the major side effects of hormonal therapy.

Nanotechnology-based delivery approaches for chemotherapeutic agents have gained immense attention in the recent past. Being a targeted form of delivery, it offers various advantages like very small size, high drug loading, ability to solubilize less water-soluble drugs, increase in bioavailability, etc. Delivering the drug in nanocarriers provides an additional opportunity to load multiple therapeutic agents at one time, making it possible to extract maximum benefit from the use of multicomponents that help to overcome the efflux mechanism of the drug, causing enhancement in drug bioavailability at the cancer site.[5] Various nanocarriers have been developed till date, including SLN, NLCs, nanoemulsions, nanoliposomes, dendrimers, polymer−lipid hybrid, nanoparticles, polymeric micelles, etc.[14] Among the mentioned nanoformulations, liposomes have been considered as the only nanotechnology-driven form that has got marketing applications.[15] These are the phospholipid-based products that form a phospholipid bilayer in aqueous solution, which allows the encapsulation of both lipophilic and hydrophilic moieties inside their membranous structure. Additionally, being very similar to the cellular membrane, it provides easy access to the inside of the cell, and being fabricated using the phospholipids, its biocompatibility and biodegradability are not an issue. Several marketed products that have used nanoliposomes as carriers for anticancer therapeutics delivery are available in the market, establishing their role as stable, safe, and scalable carriers. Some of the marketed nanoliposomes are Marqibo, Doxil, Caelyx pegylated liposomal, Myocet liposomal, Onivyde pegylated liposomal, Vyxeos liposomal, etc.[16]

However, conventional liposomes composed of concentric bilayers of phospholipids possess several advantages, but their short circulation half-life, low physical stability, high release rate, and sensitivity to environmental stresses and storage conditions limit their application in the controlled and targeted delivery. Several attempts have been made to reduce these inadequacies by not only functionalizing the liposomal surface but also improving the stability of liposomes. Among various natural polymers, chitosan has received greater attention owing to its nontoxic, biodegradable, permeation enhancer, and biocompatible properties. Chitosan being an adaptable polymer exerts its role in anticancer activity. Protection of liposomes by chitosan coating on their surface appears to be an important approach to improve the stability in different biological fluids, cellular uptake, and to prolong the release rate of the drug.[17]

In our present study, liposomal carriers loaded with exemestane and genistein with chitosan coating to be delivered via the oral route for the treatment of breast cancer were prepared. We aimed at improving the efficacy of the therapeutic moiety by maintaining a sustained rate of action while reducing the toxicity to the minimal. The optimized formulation was extensively characterized for various parameters such as particle size, entrapment efficiency, transmission electron microscopy (TEM), *in vitro*, *ex vivo*, and cell line studies.

2. MATERIALS AND METHODS

2.1. Chemicals and Reagents. *2.1.1. Drug and Excipient Procurement.* Exemestane (anhydrous form) was granted as a gift sample by Coral Drugs Private Limited (New Delhi, India). Genistein was a gift sample provided by DSM Nutritional Products Europe Ltd. Phospholipid (Lipoid S 100) was a gift sample generously offered by Lipoid GmbH, Germany. Cholesterol was gifted by Central Drug House Pvt Ltd. Delhi. Chitosan was obtained from Sigma-Aldrich (St. Louis, MO). Tween 80 was procured from Mana Scientific Products, Hyderabad, Telangana. Distilled deionized water was prepared with the Milli-Q water purification system (Millipore, Bedford, MA). MCF-7 cells were obtained from the National Centre for Cell Science, Pune, India. All additional solvents, compounds, and reagents used in the entire methods were of analytical grade.

2.2. Analytical Method Development and Validation. EXE and GEN were alienated on a reverse-phase (RP) C18 column (150 mm × 4.6 μ, 5 μ) at their respective wavelengths, i.e., 245 nm for EXE and 270.5 nm for GEN. (Using our in-house-developed method) The mobile phase comprises A—methanol:water with formic acid (0.01%), and B—acetonitrile (A:B-30:70, v/v) in an isocratic mode with a 1.0 mL/min flow

https://doi.org/10.1021/acsomega.3c09948
ACS Omega 2024, 9, 9735−9752

Table 1. Independent Variables and Their Responses of Recommended Formulations by the Design Expert Software

run	factor 1 (A): phospholipid concentration (mg)	factor 2 (B): cholesterol concentration (mg)	factor 3 (C): sonication time (min)	response 1 (R_1): particle size (nm)	response 2 (R_2): PDI	response 3 (R_3): EXE entrapment efficiency (%)	response 4 (R_4): GEN entrapment efficiency (%)
1	200	200	1	215.1	0.29	78.4	77.6
2	200	150	2	139.2	0.36	74.9	73.8
3	300	150	1	295.4	0.64	80.2	77.4
4	200	100	1	120.3	0.38	77.5	76.7
5	100	200	2	135.6	0.17	66.6	66.8
6	300	200	2	298.1	0.37	82.3	80.8
7	100	150	3	120.5	0.51	63.1	61.3
8	200	150	2	127.3	0.29	75.3	74.8
9	200	200	3	129.2	0.32	73.3	72.8
10	300	100	2	216.9	0.35	80.6	79.8
11	200	150	2	129.4	0.31	75.8	74.1
12	200	100	3	122.1	0.32	75.2	74.9
13	200	150	2	138.4	0.29	75.4	74.2
14	100	100	2	118.1	0.28	70.3	70.2
15	100	150	1	119.2	0.39	68.3	70.6
16	300	150	3	193.6	0.53	77.5	78.6
17	200	150	2	146.4	0.38	75.3	74.7

rate for the separation of both analytes. EXE and GEN when analyzed concomitantly demonstrated separation at retention times of 2.10 and 1.67 min, respectively. Additionally, the drug encapsulated in the prepared liposome formulation was also determined using the high-performance liquid chromatography (HPLC) technique, indicating that no significant changes in retention times were observed, assuring the selectivity and high specificity of the developed method.[18]

2.3. Formulation Development. *2.3.1. Preparation of Uncoated Liposomes.* Drug-loaded liposomes (EXE-GEN-LIPO) were prepared by employing phospholipid (Lipoid S 100) and cholesterol (2:1 ratio) by an ethanol injection method. Phospholipid (200 mg) and cholesterol (100 mg) were appropriately weighed and dissolved in ethanol. EXE (7.5 mg) and GEN (15 mg) were added to the organic phase. The resulting organic phase was injected dropwise to 20 mL of distilled water containing TWEEN 80 as surfactant under magnetic stirring. Incorporation of an ethanolic solution in the aqueous phase resulted in spontaneous liposome formation. To remove the traces of solvent, the liposome suspension was then kept under stirring for 1 h at room temperature followed by ultrasonication via the probe sonicator for 1 min.

2.3.2. Preparation of Chitosan-Coated Liposome. Chitosan-coated liposomes loaded with EXE-GEN (CS-EXE-GEN-LIPO) were prepared by coating the prepared liposome suspension. The chitosan solution was prepared by dissolving 0.1% w/v of chitosan to 20 mL of water with 1% acetic acid. The chitosan solution was added dropwise to the same volume of liposome solution with continuous stirring. Ultracentrifugation was performed for 1 h at 35000 rpm, and chitosan-coated liposomes emerged as pellets at the bottom of the tube, whereas an excess of chitosan appeared in the aqueous supernatant. The coated liposomes were then stored at 4 °C in a refrigerator for further use.

2.4. Formulation Design and Optimization. With the help of Design Expert software version-13.0.5.0 from StatEase (Minneapolis), process optimization was carried out using experimental designs. In the present work, Box−Behnken design (BBD) with three independent factors (A, total % phospholipid; B, total % cholesterol; and C, total % cholesterol sonication time) determined from preliminary tests and four dependent factors (R_1: particle size; R_2: polydispersity index (PDI), R_3: entrapment efficiency of EXE; and R_4: entrapment efficiency of GEN) was selected so that the most suitable formulation with projected particle size, PDI, and entrapment efficiency was obtained. With an equivalent number of tests performed, BBD has fewer design points when compared to central composite designs (CCD) and hence is less expensive. To limit the experimental error and to select the suitable model, 17 different designs of the runs were executed as shown in Table 1.

The developed polynomial equation from the Box−Behnken design is given below in eq 1:

$$R = b_0 + b_1A + b_2B + b_3C + b_{12}AB + b_{13}AC + b_{23}BC + b_{11}A^2 + b_{22}B^2 + b_{33}C^2 \quad (1)$$

In this equation, R symbolizes the response related to each factor; b_0 is the intercept or constant; b_1, b_2, and b_3 denote the linear coefficients; b_{12}, b_{13}, and b_{23} are the interaction coefficients; b_{11}, b_{22}, and b_{33} are the quadratic coefficients generated from the experimental runs; A, B, and C denote the coded levels of independent variables; and A^2, B^2, and C^2 represent the interaction as well as the quadratic terms.

2.5. Characterization of Nanoformulation. *2.5.1. Particle Size and ζ-Potential Distribution.* The vesicle size, polydispersity index (PDI), and ζ-potential of the developed formulations were determined by the dynamic light scattering technique (DLS) using Malvern Zetasizer Nano (Malvern Instrument Ltd., Malvern, U.K.). Samples were diluted with Millipore water to obtain a uniform dispersion and analyzed after vortexing. With the help of Malvern version software (Zetasizer v 6.01), analysis was performed at a temperature of 25 °C and an angle of 90°. Mean values were calculated after performing the analysis three times for each sample. The hydrodynamic diameter (z-average value) and size distribution (PDI) of blank liposomes (without drug), EXE-GEN-loaded liposomes, and chitosan-coated EXE-GEN liposomes (CS-EXE-GEN-LIPO) were examined.

The magnitude of the electrostatic or charge repulsion/attraction between particles was determined by the ζ-potential. EXE-GEN-LIPO and CS-EXE-GEN-LIPO after diluting with

https://doi.org/10.1021/acsomega.3c09948
ACS Omega 2024, 9, 9735−9752

Millipore water were placed in the electrophoretic cell. The same zetasizer instrument that was used to determine the particle size was utilized to determine the ζ-potential of the formulation. Each sample was measured three times to obtain an average of the surface charge.

2.5.2. Determination of Drug Encapsulation. By separating the unencapsulated drug from the liposomes by centrifuging 2 mL of drug-loaded EXE-GEN-LIPO (Sigma 3K30, Germany) for 1 h at 4 °C, drug encapsulation of EXE-GEN-LIPO and CS-EXE-GEN-LIPO was determined. The unentrapped drug in the supernatant was removed and filtered through a 0.2 μ nylon filter. The resulting pellets were washed with Milli-Q water twice, dissolved in ethanol, and then analyzed for quantification of the drug using our in-house-developed HPLC method. The entrapment efficiency (in % w/w) was calculated as follows:

$$\text{entrapment efficiency} = \frac{m_{\text{drug,total}} - m_{\text{drug,free}}}{m_{\text{drug,total}}} \times 100 \quad (2)$$

where $m_{\text{drug,total}}$ is the total amount of drug and $m_{\text{drug,free}}$ is the amount of free drug. The drug loading (in % w/w) was calculated as follows:

$$\text{drug loading} = \frac{m_{\text{drug,total}} - m_{\text{drug,free}}}{m_{\text{lipids,total}}} \times 100 \quad (3)$$

where $m_{\text{lipids,total}}$ is the total amount of lipids added.

2.5.3. Electron Microscopy Analysis. Transmission electron microscopy (TEM; TOPCON002B; Tokyo, Japan) was used to determine the morphological characteristics of EXE-GEN-loaded liposomes and chitosan-coated EXE-GEN liposomes by employing a negative staining method. Samples were diluted prior to placing them on a 200-mesh copper grid coated with carbon followed by staining with a drop of 2% (w/v) phototungstic acid solution. Samples were dried at room temperature, and thereafter images were recorded after a film of liposome was formed over the grid.

2.5.4. Fourier Transform Infrared (FTIR) Spectroscopy. FTIR spectra of pure (EXE, GEN, phosphatidylcholine, and cholesterol) and optimized lyophilized formulations (EXE-GEN-LIPO and CS-EXE-GEN-LIPO) were recorded to identify the possibility of any interaction between the drug and the excipients used in the liposome formulation using the KBr press method (FTS-135, Biorad). The spectra recorded were further analyzed by scanning between 400 and 4000 cm^{-1}.

2.5.5. X-Ray Diffraction (XRD) Study. The polymorphic structure change of the drug in the formulation was inspected by an X-ray-based diffraction instrument model (Rigaku Miniflex 600; Japan). The crystallinity of the formulated liposomes was measured by X-ray at 2θ values of 5−80° by keeping the rate of analysis at 4°/min. XRD spectra were recorded and evaluated. The physical states of EXE, GEN, cholesterol, chitosan, and optimized CS-EXE-GEN-LIPO were investigated by this technique.[19]

2.5.6. Differential Scanning Calorimetry. In this study, a lyophilized sample of liposome (5 mg) was placed on the aluminum pans and then preserved hermetically, whereas an empty pan was taken as a reference. For maintaining an inert environment around the sample holder, nitrogen gas was regulated at a flow rate of 50 mL/min; however, the sample was gradually heated at a rate of 10 °C/min using the differential scanning calorimetry (DSC) model (PerkinElmer; Software version, Pyris 6.0). In this thermal-based analysis, information associated with the amount of energy either absorbed or emitted by the samples was examined.[20]

2.6. *In Vitro* Drug Release Study. The dialysis bag method was performed to evaluate the release pattern of drugs from EXE-SUSP, GEN-SUSP, EXE-GEN-SUSP, EXE-GEN-LIPO, and CS-EXE-GEN-LIPO. For replicating the blood circulation condition, simulated gastric fluid (pH 1.2) for 2 h and simulated intestinal fluid (pH 6.8) for 24 h were taken as the release media. 3 mL of the entire sample formulations cited above were kept in the dialysis bag having a molecular weight cutoff, 12 kDa (Sigma), plunged in the glass beaker having a release media (100 mL) with 1% Tween 80 for assisting solubilization and maintaining sink conditions. The shaker incubator was maintained at normal physiological temperature (37 ± 0.5 °C) with continuous shaking, and the dialysis bag placed in the beaker containing the release media was positioned inside the shaker incubator. To maintain the sink conditions, an equal volume of fresh medium was added prior to withdrawing the samples (2 mL) at fixed time intervals through a side tube up to a period of 24 h. By using the validated HPLC method, the withdrawn samples collected were filtered by a 0.45 mm filter and analyzed. The study was repeated at least three times, and then the concluding outcomes were reported as average. The release data (pH 6.8) were fitted into various kinetic models such as zero-order, first-order, Higuchi kinetics, Korsmeyer-Peppas model, and Hixon−Crowell model. The correlation coefficient with maximum value (R_2) was taken as the best-fit model.

2.7. Statistical Analysis. Each experiment was performed in triplicate and the obtained outcomes of the experiments were represented as mean ± standard deviation (SD). Using GraphPad Prism version 8.0.2. statistical analysis of the data were performed and $p < 0.05$ was regarded as statistically significant and statistical differences were evaluated by one-way analysis of variance (ANOVA) followed by Tukey's multiple comparisons test.[21]

2.8. Animal Studies. Albino female Wistar rats weighing 200−250 g were received from the Central Animal House Facility, Jamia Hamdard, New Delhi with prior approval from the Institutional Animal Ethics Committee (Approval No. 1754). All of the experiments were performed in compliance to the guidelines issued by the Committee for the Purpose of Control and Supervision of Experiments on Animals (CPCSEA).The animals were housed in polypropylene cages adapted under standard laboratory 25 ± 2 °C relative humidity at 50−60% with free water access.

2.8.1. Ex Vivo Intestinal Permeation Studies. The intestinal permeation study was executed to determine the apparent permeation of both drugs from EXE-GEN-SUSP, EXE-GEN-LIPO, and CS-EXE-GEN-LIPO by the noneverted gut sac model using female Wistar rats.

The intestine was surgically removed after sacrificing the female Wistar rats fasted overnight by cervical dislocation subsequent to anesthetizing the rats intraperitoneally using a combination of ketamine and xylazine. Waste material was removed by separating and rinsing the ileum segments with saline. With the help of a blunt needle, standardized doses of EXE-GEN-SUSP, EXE-GEN-LIPO, and CS-EXE-GEN-LIPO individually were loaded into the intestinal mucosal sac and both sides of the sac were tightly threaded. A Tyrode solution prewarmed to 37 ± 0.5 °C in a jacketed glass with continuous flow of hot water in the jacket and oxygenated through an

https://doi.org/10.1021/acsomega.3c09948
ACS Omega 2024, 9, 9735−9752

aerator with 95% aqueous O_2 for 2 h was used to suspend the sac containing the drug and formulation. Fresh Tyrode solution of an equivalent quantity was refilled after the samples were withdrawn from the acceptor segment at a preset time interval. Using the HPLC method as mentioned, earlier samples were diluted, collected, filtered, and analyzed for the drug concentration.[22]

The apparent permeability of the drug (P_{app}, in cm/min) was computed by the following formula:

$$P_{app} = \frac{F}{A} C_0 \tag{4}$$

where F signifies the permeation flux (mg/cm^2/min), A represents the total surface area of the tissue (cm^2), and C_0 symbolizes the initial concentration of the drug present in the mucosal sac (μg/mL).

2.8.2. Confocal Laser Scanning Microscopy (CLSM) Study. Intestinal uptake assessment was carried out on female Wistar rats fasting for 24 h. The elongated part of the ileum after sacrificing was obtained and cleaned with Tyrode's buffer to eradicate fecal matter. Fluorescent dye Rhodamine B (0.03%) was incorporated into the optimized CS-coated LIPO without drugs and a clear Rhodamine B solution. Rhodamine B-labeled CS-coated LIPO and the solution were inserted with the help of a syringe into separate sacs, and both the ends of the sac were tightly closed followed by immersing them in 200 mL of Kreb's buffer for 3 h maintained at 37 ± 2 °C with 45 rpm and 95% of the O_2 supply. The intestinal sac was then untied after 3−4 h and a surfeit of dye was washed with normal saline. Small pieces of tissues were mounted on different slides and analyzed by CLSM (CLSM: Olympus Fluoview FV 1000) for determining the intensity of penetration besides fluorescence correlation spectroscopy with 540 and 625 nm as excitation wavelength and emission wavelength, respectively.[23]

2.8.3. Acute Toxicity Studies. The pharmacological safety of the prepared liposomes was evaluated by acute toxicity studies on female Wistar rats following the guidelines of the Organization for Economic Co-operation and Development (OECD). Female Wistar rats weighing 200−250 g were selected arbitrarily and were treated with EXE-SUSP, GEN-SUSP, and CS-EXE-GEN-LIPO at their therapeutic doses of EXE (15 mg/kg) and GEN (25 mg/kg) through the oral gavage route on a daily basis for 14 days. During the study, all of the animals were scrutinized daily for different symptoms like toxicity, mortality, and behavioral aberrations, along with alteration in physical form, damage, tenderness, and signs of disease. Before the treatment and after the treatment period was over, body weight was recorded. After 14 days of treatment, rats were euthanized and the imperative organs (liver, heart, and kidneys) were assembled, cleaned with normal saline, and positioned in 10% formalin. Samples were dried out with ethanol and entrenched in paraffin blocks, and then, thin sections of 6 μm were sliced with the help of a rotary microtome (Leica Multicut 2045, Reichert-Jung Products, Wetzlar, Germany). Utilizing hematoxylin and eosin (HE) as stains, slides were stained and were studied by a light microscope (ZEISS Primostar, Oberkochen, Germany) to examine the morphological changes.[24]

2.9. Cell Line Studies. *2.9.1. Cellular Uptake Study.* Using fluorescence microscopy, the cellular uptake of liposome formulation was studied on the MCF-7 cell line. Rhodamine-loaded CS-LIPO and plain rhodamine suspensions were added to MCF-7 cells. An ultraclean coverslip was positioned in the 6-well microplate with a density of 5,000 to 10,000 cells per well in appropriate medium, propagated with MCF-7 cells, and allowed to develop for 24 h at 37 ± 2 °C in an atmosphere of 5% CO_2.[25] Each well was enhanced with 10% fetal bovine serum (FBS), 100 units/mL of penicillin, and 100 mg/mL of streptomycin followed by incubation of 24 h at 37 ± 2 °C. Then, subsequent to the accomplishment of 90% confluency, the cells were treated with rhodamine-loaded LIPO and plain rhodamine suspension and incubated for 24 h. Cell plates were washed twice with phosphate-buffered saline (PBS). Afterward, the cells were stipulated with 4% paraformaldehyde, and by utilizing 4,6-diamidino-2-phenylindole (DAPI) as staining medium, the slides were visualized by using a fluorescent upright microscope inverted laser scanning confocal microscope (ILSCM), Model: LSM900, Zeiss, Germany.

2.9.2. Cytotoxicity Study by 3-(4,5-Dimethylthiazol-2-yl)-2,5-diphenyltetrazolium Bromide (MTT) Assay. In vitro cytotoxicities of EXE-SUSP, GEN-SUSP, EXE-GEN-SUSP, EXE-GEN-LIPO, CS-EXE-GEN-LIPO, and blank LIPO were investigated by performing MTT assay. Samples were tested at different concentration ranges (6.25, 10, 25, 50, and 100 μg/mL) on the MCF-7 cells and after that, incubated for 24 h. Each well was endowed with 20 μL of MTT solution (3-(4,5-dimethylthiazol-2-yl)-2,5 diphenyltetrazolium bromide), and then, the cell plates were incubated again for 4 h at 37 °C to form purple color formazon crystals. Excess cell culture medium was removed, and the formazon crystals formed were dissolved by adding 100 μl of dimethyl sulfoxide (DMSO) solution. Enzyme-linked immunosorbent assay (ELISA) plate reader (iMark, Biorad) was utilized to record the absorbance at 570 nm. % cell cytotoxicity was calculated using the below-mentioned formula, and the untreated cells showing 100% viability were considered as control samples.

$$\%\ \text{cell cytotoxicity} = \frac{X_{control} - X_{sample}}{X_{control}} \times 100 \tag{5}$$

where $X_{control}$ refers to the absorbance of the control and X_{sample} refers to the absorbance of the sample. The IC_{50} value was estimated by GraphPad Prism 8.0.2.

2.9.3. DPPH Assay. The fundamental scavenging potentials of EXE-SUSP, GEN-SUSP, EXE-GEN-LIPO, Placebo LIPO, and CS-EXE-GEN-LIPO by 2,2-diphenyl-1-picrylhydrazyl were assessed by radical DPPH and compared to that of a standard ascorbic acid solution. A 0.04% w/v solution of DPPH in ethanol was added to 2 mL of various concentrations of EXE-SUSP, GEN-SUSP, EXE-GEN-LIPO, Placebo LIPO, and CS-EXE-GEN-LIPO. The reaction mixture was dynamically shaken and kept for 45 min in a dark area at 25 °C.[26] The absorbance of the tested samples and DPPH solutions was taken by UV spectrophotometric measurements at 517 nm. The DPPH scavenging capacity percentage was determined using eq 6, where (A) indicates the blank absorbance (control) and (B) refers to the sample absorbance with varying concentrations. The percentage inhibition versus sample concentration graph was plotted followed by estimation of the inhibitory concentration percentage (IC50) of the tested samples and IC50 of the standard ascorbic acid by GraphPad Prism 8.0.2.

$$\%\ \text{inhibition} = \frac{A_{control} - A_{sample}}{A_{control}} \times 100 \tag{6}$$

https://doi.org/10.1021/acsomega.3c09948
ACS Omega 2024, 9, 9735−9752

where $A_{control}$ is the absorbance of the control and A_{sample} is the absorbance of samples with different concentrations.

2.10. Statistical Analysis. Each experiment was performed in triplicate and the obtained outcomes of the experiments were represented as mean ± standard deviation. Using GraphPad Prism version 8.0.2, statistical analysis of the data was performed; $p < 0.05$ was regarded as statistically significant and statistical differences were evaluated by one-way ANOVA followed by "Tukey"s multiple comparisons test.[21]

2.11. Storage Stability Study. The stability parameters of the optimized lyophilized EXE-GEN-LIPO and CS-EXE-GEN-LIPO were evaluated by performing an accelerated stability study for a period of 6 months by monitoring any change in particle size, PDI, and %EE at planned time periods of 0, 1, 3, and 6 months. The lyophilized formulation was stored in amber-colored containers at 4 °C, 25 °C, 2 °C/60% RH, and 40 °C, 2 °C/75% RH in a stability chamber (Macro Scientific, Mumbai, India) followed by diluting with Milli Q water for analyzing the particle size, PDI, and % EE after 6 months.

3. RESULTS AND DISCUSSION

3.1. Preparation of the Nanoformulation. Remarkable escalation in the liposome-based delivery system carrying therapeutic agents at the preferred site with the lowest feasible impediment in tissue uptake and most significant pharmacokinetics and pharmacodynamics have been observed in the last few decades. A high drug concentration desired for accomplishing superior therapeutic index and drug resistance were the two major limitations caused by the liposome-based delivery system comprising a single therapeutic agent. In this study, liposomes were synthesized encapsulating two drugs, EXE and GEN, simultaneously in the required ratio using phosphatidylcholine, cholesterol, and TWEEN 80 by the ethanol injection method. Owing to the amphiphilic property of phosphotidylcholine, hydrophobic drugs are solubilized in the organic phase and remain entrapped in the hydrophobic bilayer region. To make liposomes more stable under aqueous conditions, one of the common additives, cholesterol, was used to improve their bilayer characteristics. The surface tension of the media was reduced by TWEEN 80, resulting in the appropriate molecular geometry and hydrophobicity for the bilayer vesicle formation due to its large hydrophilic headgroup. It acts as an edge activator on the membrane of liposomes. The ethanol injection method was used over other methods as phospholipids used in this method do not get degraded and therefore are protected from oxidation, which is not the case in the thin film hydration method. This technique employs ethanol, which is reasonably harmless unlike chloroform and methanol that are used as organic solvents in the thin film hydration technique. The stability of liposomes prepared by this method is superior and due to its safety, rapidity, and reproducible disposition, the ethanol injection technique is favorable in industrial scale for bulk manufacturing as compared to other methods of liposome preparation.[27]

Although several advantages of liposomes are stated above, additional upgrading is still necessary to augment their effectiveness as drug delivery systems. Enzymes present in the GIT and pH of GIT lead to disruption of liposomes liberating encapsulated drugs. As a result, stable liposomes in normal body milieus with sustained drug release and delivering the loaded drug to the intended target site were achieved by coating the liposomal surface with polymers. Chitosan possessing cationic, bioadhesive, biocompatible, biodegradable, and absorption-enhancer features was employed for coating the liposome surface, resulting in enhanced liposome properties by improving the bioavailability of drugs by increasing the residence time at the absorption site. On coating, chitosan having a positively charged surface binds to the negatively charged surface of liposomes through ionic interaction, leading to a prolonged and controlled release.[28]

3.2. Formulation Design and Optimization. Inclusion of independent and dependent variables in Design Expert software with BBD generated a total of 17 runs, and the effects of independent variables on the dependent variables were predicted by the 17 formulations prepared and their responses as suggested by the software. A quadratic model was established to be the most appropriate model based on the generated responses and acquired data of regression value statistically validated using ANOVA. A positive sign indicates the positive response of the independent variable on the dependent variable, while a negative sign depicts the suppressed effect of the independent variable on the dependent variable (Table 2).[29]

Table 2. Summary of Regression Analysis for R_1 (Particle Size), R_2 (PDI), R_3 (EXE Entrapment Efficiency), and R_4 (GEN Entrapment Efficiency) as Suggested by BBD

quadratic model	R^2	adjusted R^2	predicted R^2	SD	% CV
R_1	0.9948	0.9882	0.9786	6.51	4
R_2	0.9634	0.9163	0.9279	0.0319	8.77
R_3	0.9986	0.9968	0.9920	0.2877	0.3851
R_4	0.9968	0.9927	0.9761	0.4141	0.5591

The polynomial equations generated by the Design Expert software are as mentioned below:

$$R_1 = +136.14 + 63.83A + 25.08B - 23.08C + 15.92AB - 25.77AC - 21.92BC + 45.77A^2 + 10.27B^2 + 0.2675C^2 \quad (7)$$

$$R_2 = +0.3260 + 0.0675A - 0.0225B - 0.0025C + 0.0325AB - 0.0575AC + 0.0225BC + 0.0783A^2 - 0.1118B^2 + 0.1132C^2 \quad (8)$$

$$R_3 = +75.34 + 6.54A - 0.3750B - 1.91C + 1.35AB + 0.6250AC - 0.7000BC - 2.11A^2 + 1.72B^2 - 0.9575C^2 \quad (9)$$

$$R_4 = +74.32 + 5.96A - 0.4500B - 1.84C + 1.10AB + 2.62AC - 0.7500BC - 1.72A^2 + 1.80B^2 - 0.6225C^2 \quad (10)$$

3.2.1. Effect of Independent Variables on Particle Size. As depicted in Table 1, all of the 17 runs that were generated by the Design Expert software exhibited particle sizes in the range of 118.1−298.1 nm. On increasing the concentration of phospholipid, the particle size increased, whereas with increasing surfactant concentration and sonication time, particle size decreased according to the plots shown in Figure 1A and the polynomial equation generated. Owing to the viscosity of the dispersion medium at high lipid concentrations,

https://doi.org/10.1021/acsomega.3c09948
ACS Omega 2024, 9, 9735−9752

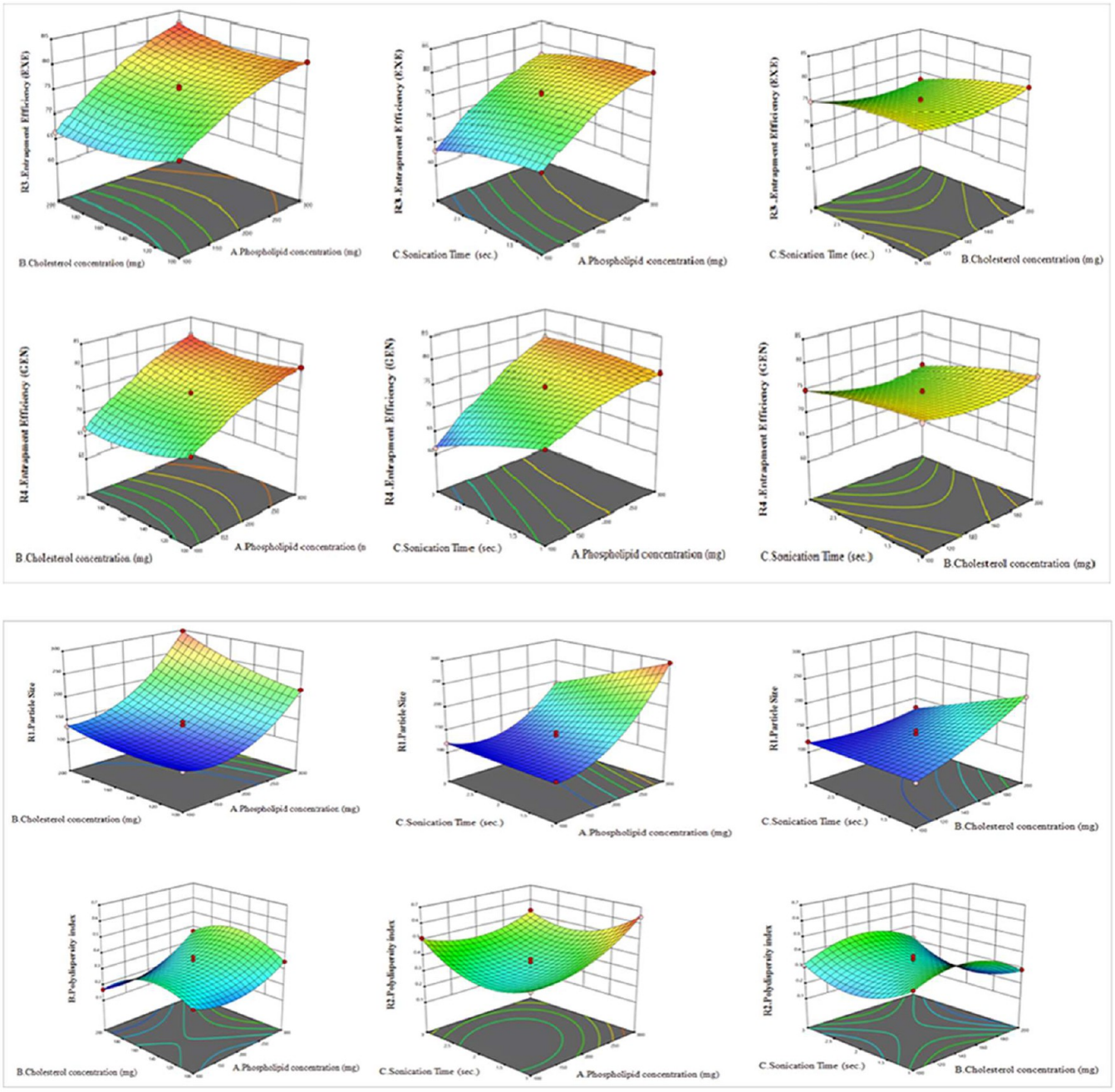

Figure 1. Representation of three-dimensional plots displaying the effect of different independent variables on (A) particle size, (B) PDI, (C) % entrapment efficiency of EXE, and (D) % entrapment efficiency of GEN.

the particle size is increased at higher lipid concentrations. On increasing the sonication time, the particle size reduces as the sonication energy utilized in the preparation of liposomes breaks down the coarse particles to nanorange. As the contact angle between the aqueous phase and the lipid phase gets reduced on increasing the surfactant concentration, the particle size is decreased.

3.2.2. Effect of Independent Variables on PDI. The PDI of all of the runs generated by Design Expert software was observed to be in the range of 0.17−0.64 according to Table 1. According to the three-dimensional (3D) plots as depicted in Figure 1B and the polynomial equation generated, PDI increases as the phospholipid concentration is increased and decreases as the surfactant amount and sonication time are increased. PDI plays a significant role in the stability of liposomes. A smaller PDI value signifies a homogeneous distribution of particles. Owing to the formation of a viscous emulsion at increased phospholipid concentration, a higher sonication energy is required to break all the particles, thereby increasing the PDI value. However, by increasing the sonication time, the energy related with it also increases, resulting in a breakdown of particles and thus generating homogeneously distributed particles. In the same way, on increasing the surfactant concentration, the PDI value is decreased as the interfacial tension is reduced by the surfactant, thus lessening the droplet size and consequently resulting in the eminent homogeneity.[30]

https://doi.org/10.1021/acsomega.3c09948
ACS Omega 2024, 9, 9735−9752

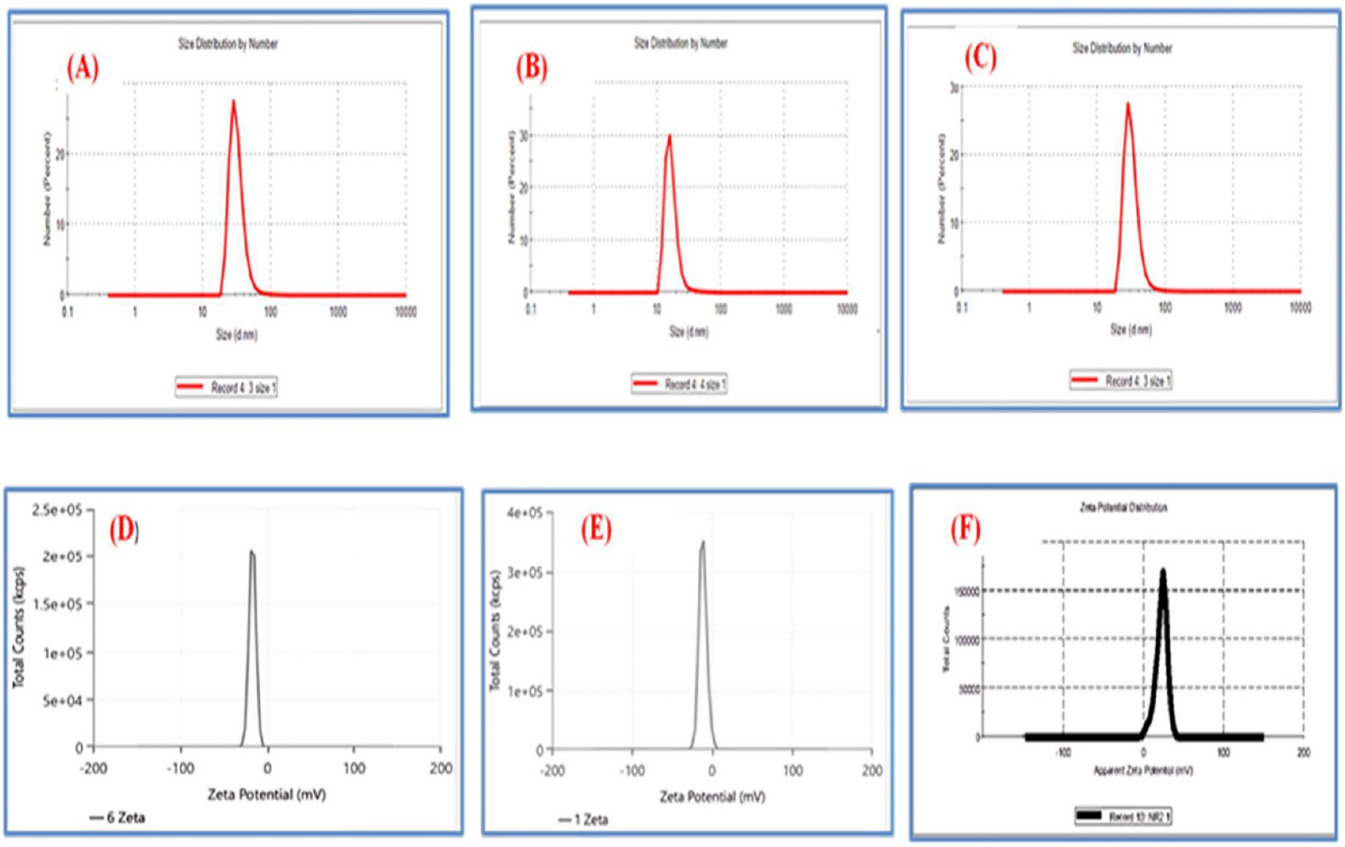

Figure 2. Particle size distribution of (A) placebo LIPO, (B) EXE-GEN-LIPO, (C) CS-EXE-GEN-LIPO, and ζ-potential of (D) placebo LIPO, (E) EXE-GEN-LIPO, and (F) CS-EXE-GEN-LIPO.

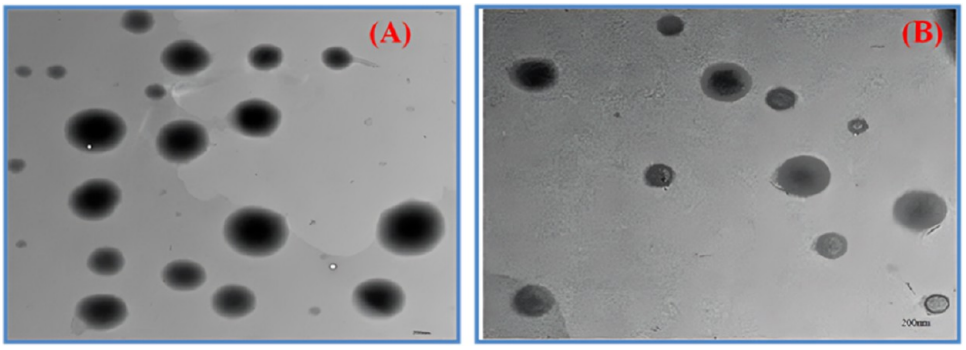

Figure 3. TEM micrographs of (A) optimized EXE-GEN-LIPO and (B) CS-EXE-GEN-LIPO (scale bar: 200 nm).

3.2.3. Effect of Independent Variables on % entrapment efficiency (Y_3 and Y_4). With the help of Design Expert software, the entrapment efficiency of EXE and GEN was obtained in the range of 61.3−82.3%. From Figure 1C,D, it was concluded that on increasing the phospholipid concentration, the entrapment efficiency of both EXE and GEN was considerably increased, while by augmenting the sonication time and surfactant concentration, the entrapment efficiency was decreased. Since the phospholipid concentration employed in the formulation increased, more amount of drugs can accommodate in the space available and a lesser amount of drug migrates to the aqueous phase, thus increasing the entrapment efficiency.

3.3. Characterization of Formulated Liposomes. *3.3.1. Particle Size, PDI, and ζ-Potential.* The particle size, PDI, and ζ-potential of all of the liposomal formulations were measured to authenticate the development of a stable product of appropriate quality. From Figure 2A, it can be observed that the particle size of blank liposomes is 88.42 ± 1.9 nm with a PDI of 0.402, which increased to 104.6 ± 3.8 nm with a PDI of 0.399 (Figure 2B) when both the drugs (EXE and GEN) were loaded into the formulation. Increase in the size was predictable owing to the inclusion of the drug into the core of the particles. The particle size of chitosan-coated liposomes was considerably increased to 120.3 ± 6.4 nm with a PDI of 0.381 (Figure 2C). A PDI value more than 0.5 signifies that the particles are not homogeneously distributed; as a result, low PDI values are required to attain uniformly distributed particles.

ζ-Potential is an additional factor that has a role in the stability of encapsulation systems and electrostatic interactions. The ζ-potential for blank liposomes, EXE-GEN-LIPO, and CS-

https://doi.org/10.1021/acsomega.3c09948
ACS Omega 2024, 9, 9735−9752

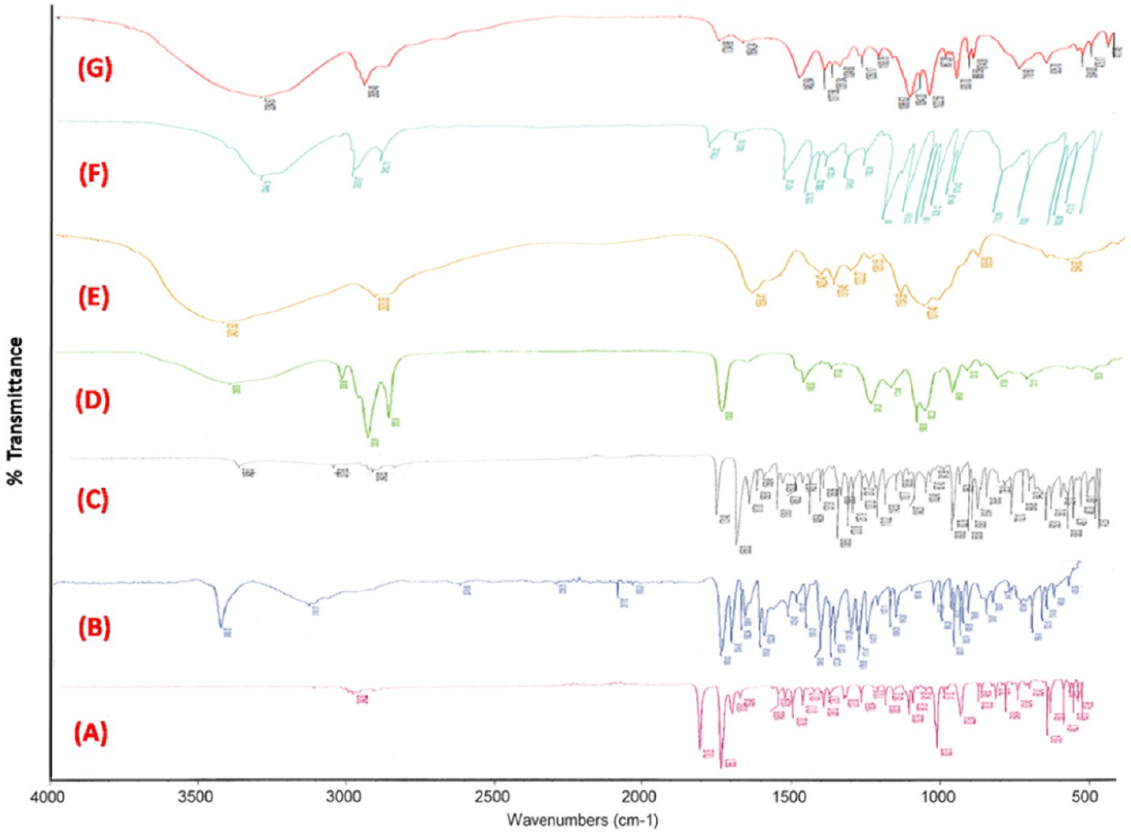

Figure 4. FTIR spectra of (A) EXE, (B) GEN, (C) physical mixture of drugs (EXE + GEN), (D) phospholipid, (E) chitosan, (F) optimized EXE-GEN-LIPO, and (G) optimized CS-EXE-GEN-LIPO.

EXE-GEN-LIPO was found to be −16.54, −16.56, and +22.4, respectively (Figure 2D−F). The negative value of ζ-potential in the liposomal formulations is ascribed to the phosphatidic acid groups of phospholipids. Subsequently, on coating with chitosan, owing to the free amine groups present in the chitosan, it binds to the negatively charged surface of the liposomes, thereby changing the surface charge of liposomes to positive, which results in higher repulsive forces, preventing the aggregation of particles and leading to higher stability.[31]

3.3.2. Encapsulation Parameter Determination. The entrapment efficiency of EXE and GEN in CS-EXE-GEN-LIPO was found to be 77.5 ± 3.3 and 76.5 ± 3.2%, respectively, with no significant difference in the drug entrapment efficiency of EXE and GEN when compared to noncoated liposomes (76.8 ± 2.9 and 74.56 ± 2.1, respectively). The drug loadings were found to be 2.12 ± 0.4 and 3.81 ± 0.9. This result signifies the potential of the formulation for withholding bioactive compounds in the bilayer membrane or the central core of liposomes. Further, the value of drug encapsulation and drug loading demonstrated that on storage variation was not observed.[32]

3.3.3. Morphological Characteristics of the Formulated Optimized Liposomes. The morphological study of liposomes under TEM analysis revealed that the particles of liposomes were homogeneously distributed and are spherical in shape as demonstrated in Figure 3A,B. No aggregation was observed in the EXE-GEN-LIPO and CS-EXE-GEN-LIPO formulations and all of the results were consistent with the results obtained by DLS. The TEM images revealed the interior core, signifying the drugs entrapped, with the exterior layer of phospholipid depicted by light periphery. In CS-EXE-GEN-LIPO, a thin layer was observed on the surface of liposomes due to the interaction of the phospholipid with chitosan, thus forming an obstruction to the liposomal surface enhancing their colloidal stability in excess water and sustaining the loaded drug release.

3.3.4. FTIR Analysis of the Prepared Liposomes. FTIR spectral analysis was carried out to evaluate any probable interaction among drugs and the excipients used in the formulation of liposomes (Figure 4). The pure drug EXE demonstrated a sturdy distinctive peak at 2942.82 cm^{-1} subsequent to C−H stretching, 1731.35 cm^{-1} corresponding to C═O stretching, 1656.71 cm^{-1} corresponding to C═C stretching, and 902.76−623.45 cm^{-1} corresponding to C−H bending. Pure GEN illustrated the existence of a distinctive peak at 3409.55 cm^{-1} corresponding to O−H stretching, 3101.37 cm^{-1} corresponding to aromatase C−H stretching, 1650.42 cm^{-1} corresponding to C═O stretching, and 1308.0−1143.73 cm^{-1} corresponding to C═O═C stretching.

In addition, phosphatidylcholine showed the presence of distinct peaks at 2922.81 and 2852.99 cm^{-1} corresponding to the C−H stretching band of a long fatty acid chain. The peaks at 1735.08, 1241.29, and 1062.23 cm^{-1} correspond to the carbonyl stretching band in the fatty acid ester, P═O stretching band, and P−O−P stretching band, respectively. Furthermore, chitosan showed the presence of distinct peaks at 3431.93 and 2923.06 cm^{-1} corresponding to the O−H bond stretching and C−S group stretching. The peaks at 1654.41, 1154.56, and 1017.40 cm^{-1} correspond to the N−H bending, asymmetric C−O−C stretching, and C−O vibrations, respectively. The peaks of 3244.19, 2933.87, 1735.02, 1653.19, 1457.26, and 1396.71 cm^{-1} belonging to lyophilized EXE-GEN-LIPO were observed to be shifted in lyophilized

https://doi.org/10.1021/acsomega.3c09948
ACS Omega 2024, 9, 9735−9752

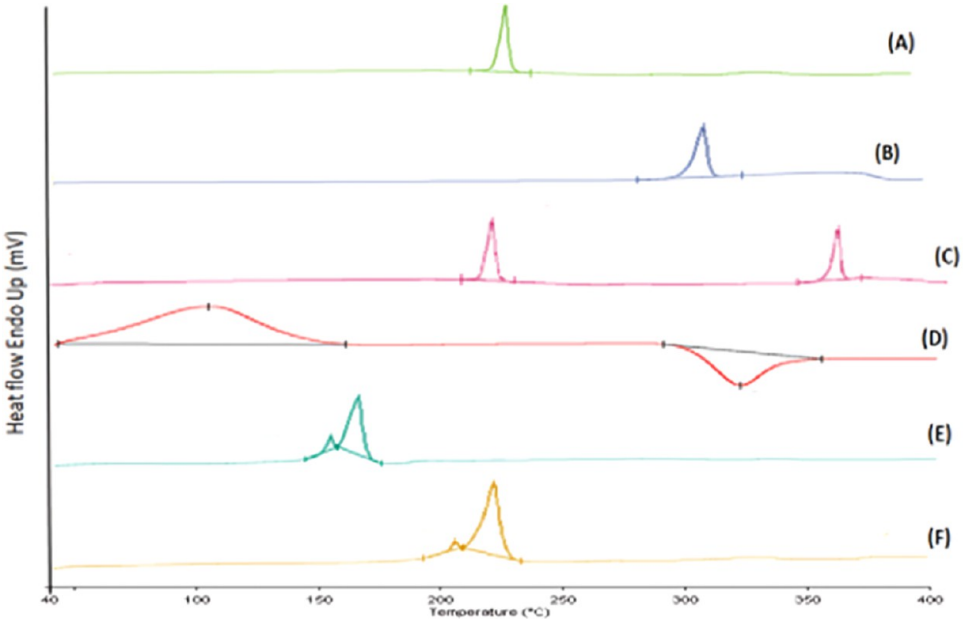

Figure 5. DSC thermogram of (A) EXE, (B) GEN, (C) physical mixture of drugs (EXE + GEN), (D) chitosan, (E) lyophilized formulation of EXE-GEN-LIPO, and (F) lyophilized formulation of CS-EXE-GEN-LIPO.

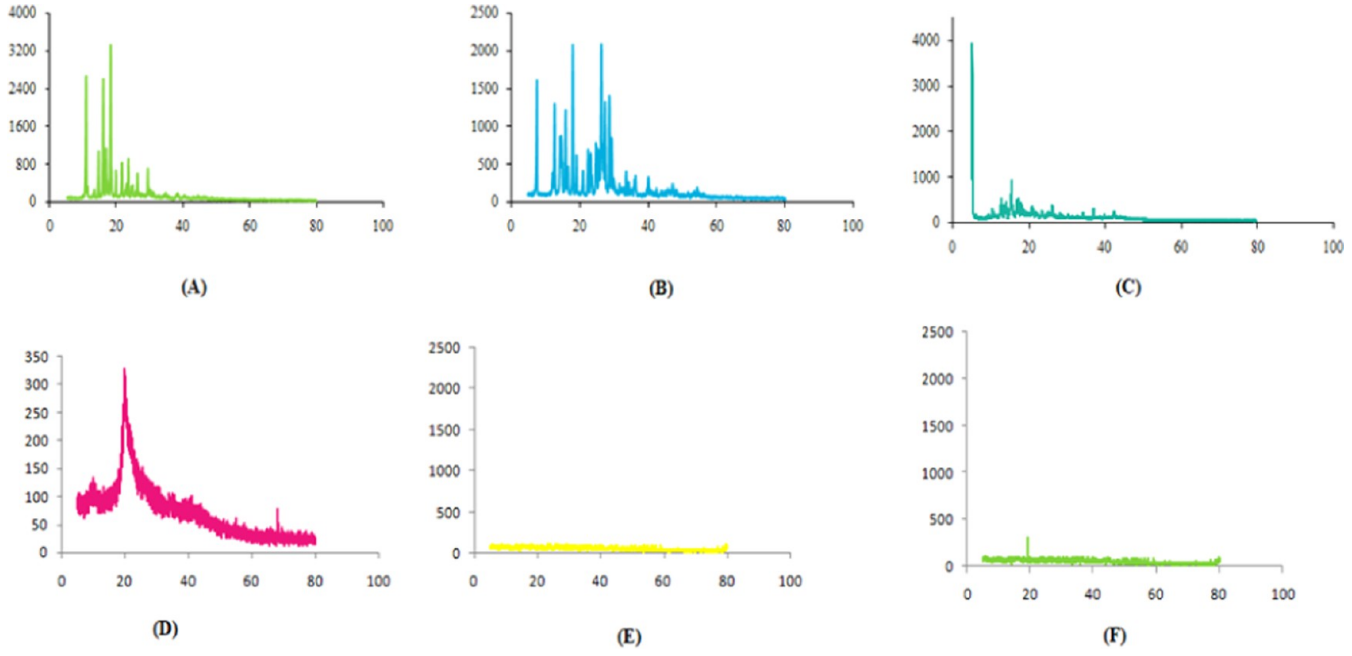

Figure 6. XRD spectra of (A) EXE, (B) GEN, (C) cholesterol, (D) chitosan, (E) lyophilized formulation of EXE-GEN-LIPO, and (F) lyophilized formulation of CS-EXE-GEN-LIPO.

CS-EXE-GEN-LIPO, signifying the formation of new non-covalent bonds such as "H" bonds or strengthening of H bonds assisting the effectual solubilization and entrapment of beneficial agents within liposomes, consequently validating successful chitosan coating on the liposomes.

3.3.5. DSC Analysis. The effects of temperature on the physical mixtures of drugs (EXE + GEN), EXE-GEN-LIPO and CS-EXE-GEN-LIPO, were examined by the DSC study, as illustrated in Figure 5. The EXE and GEN thermogram shows a sharp endothermic peak at 198.552 and 307.488 °C, respectively, revealing its melting point. Chitosan has an anarchic configuration with a strong magnetization for water and as a result gets easily hydrated when present in solid form. Chitosan showed an endothermic peak at 104.210 °C resulting from loss of water related with the hydrophilic group of chitosan and an exothermic peak at 315.831 °C. EXE-GEN-LIPO showed two peaks: one at 169.223 °C representing the mannitol peak and another small peak at 158.151 °C corresponding to the cholesterol peak, whereas the peaks of EXE and GEN completely disappeared due to the modification of both drugs from crystalline to amorphous form, signifying that both the drugs were homogeneously dispersed during the liposome preparation. When compared to EXE-GEN-LIPO, the CS-EXE-GEN-LIPO thermogram showed two peaks, one

https://doi.org/10.1021/acsomega.3c09948
ACS Omega 2024, 9, 9735−9752

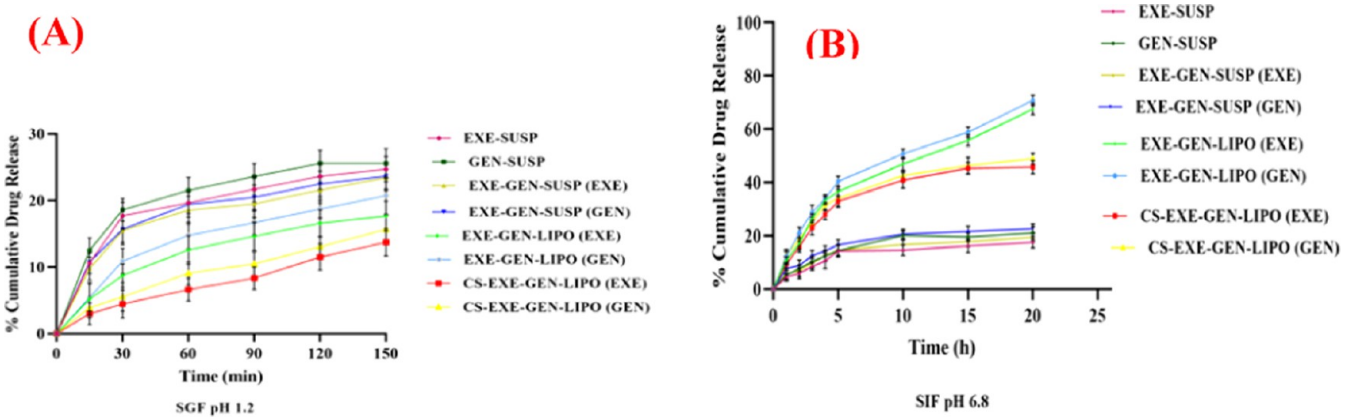

Figure 7. *In vitro* drug release profiles of EXE and GEN from EXE-SUSP, GEN-SUSP, EXE-GEN-SUSP, EXE-GEN-LIPO, and CS-EXE-GEN-LIPO at (A) pH 1.2 and (B) pH 6.8. The values are expressed as mean ± SD, n = 3.

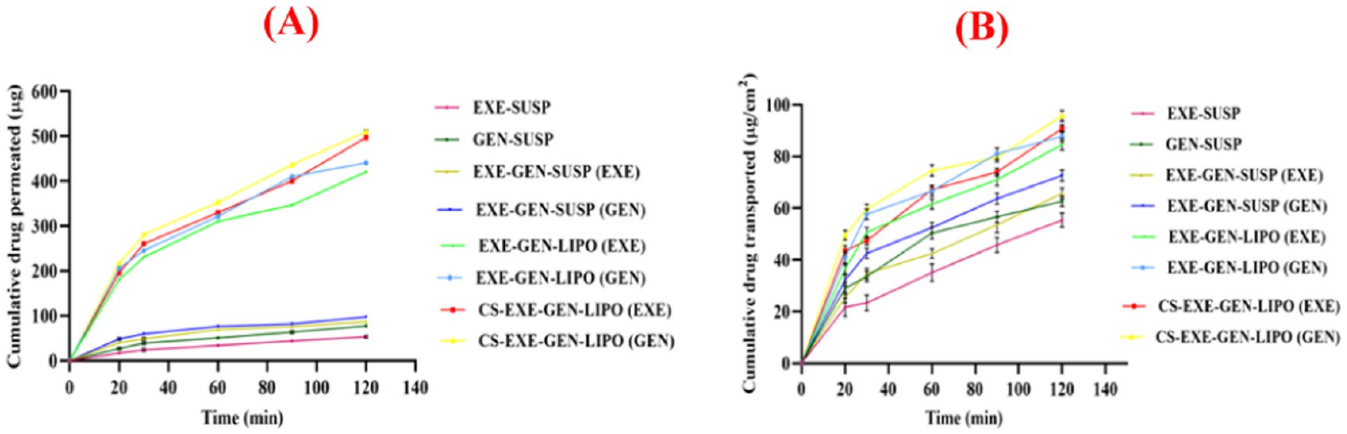

Figure 8. *Ex vivo* intestinal permeation study demonstrating (A) cumulative amount of drug permeated (μg) versus time (min) and (B) cumulative amount of drug transported (μg/cm^2) with time (min).

at 170.988 °C with ΔH 659.46 J/g and a small peak at 158.93 °C with ΔH 26.567 J/g. The ΔH of the coated liposomes (CS-EXE-GEN-LIPO) was observed to be increased when compared with the uncoated liposomes (EXE-GEN-LIPO), affecting the membrane fluidity of liposomes and thus improving the thermal stability of CS-EXE-GEN-LIPO owing to the layer modification by chitosan coating.[33] Moreover, the results of DSC also indicated that there was no chemical interaction between the drug and the excipients.

3.3.6. XRD Analysis. XRD analysis further confirms the DSC results of the samples under examination. To examine the crystallinity of pure EXE, GEN, and the excipients used in the preparation of liposomes, X-ray diffraction study was carried out, and the scattering pattern as depicted in Figure 6 was obtained for EXE, GEN, and lyophilized liposome formulation. The diffractogram pattern of pure EXE and GEN showed sharp characteristic peaks demonstrating the crystalline nature of the drug. The cholesterol diffractogram pattern shows a sharp crystal reflection. The diffractogram pattern of chitosan shows peaks of stronger intensity representing the semicrystalline nature of chitosan. However, the absence of sharp peaks and the presence of broad peaks were observed for the lyophilized EXE-GEN-LIPO and CS-EXE-GEN-LIPO due to the cryoprotectant mannitol used, evidently indicating the transformation of drug from crystalline to amorphous form and complete encapsulation of both drugs in the lipid formulation.

3.4. *In Vitro* Drug Release Study. A partial description of the residence time of a drug is mimicked by an *in vitro* release study. The *in vitro* release profiles of EXE and GEN from EXE-SUSP, GEN-SUSP, EXE-GEN-SUSP, uncoated liposomes, and chitosan-coated liposomes were determined in phosphate-buffered saline (PBS) at two different pH conditions (pH 1.2 and 6.8) at 37 °C as depicted in Figure 7. In a simulated gastric media of pH 1.2, EXE and GEN release from EXE-SUSP, GEN-SUSP, EXE-GEN-SUSP, and EXE-GEN-LIPO was found to be 24.70 ± 1.9, 25.58 ± 1.2, 17.67 ± 1.5, 23.66 ± 1.3, 17.67 ± 1.4, and 20.73 ± 1.3%, respectively. However, the release of EXE and GEN from CS-EXE-GEN-LIPO was merely 13.73 ± 1.12 and 15.66 ± 1.8%, respectively, signifying that majority of the drug remained entrapped surrounded by the lipid matrix shielding the drug from degradation that might possibly occur in the stomach, whereas in a simulated intestinal fluid of pH 6.8, EXE and GEN release from EXE-SUSP, GEN-SUSP, EXE-GEN-SUSP, and EXE-GEN-LIPO displayed a release of 21.03 ± 1.3, 17.52 ± 1.4, 19.47 ± 1.5, 22.66 ± 1.2, 67.55 ± 1.6, and 70.77 ± 1.5% respectively. The rapid release of EXE and GEN from EXE-GEN-LIPO could be due to the fast desorption of the surface-bound drug. As the initial burst release does not guarantee constant delivery at the target site, liposomes were coated with a hydrophilic polymer, i.e., chitosan, for sustained release of drugs. EXE and GEN in CS-EXE-GEN-LIPO showed a sustained release of 45.83 ± 1.5 and 48.98 ± 1.3%, respectively, owing to surface coating that

https://doi.org/10.1021/acsomega.3c09948
ACS Omega 2024, 9, 9735−9752

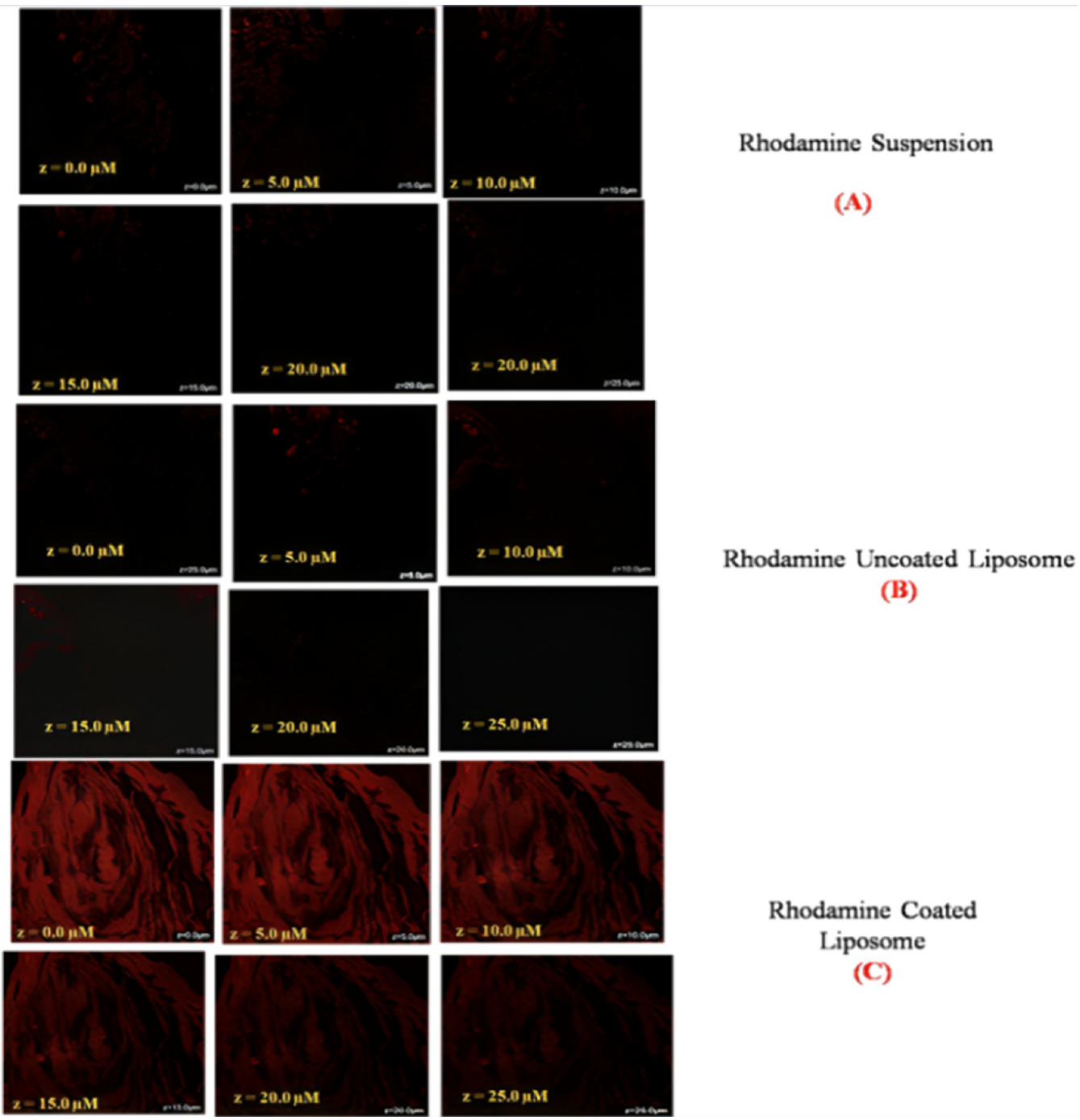

Figure 9. CLSM images of small intestine for determining the depth of penetration of (A) Rhodamine B, (B) Rhodamine B-labeled uncoated liposome, and (C) Rhodamine B-labeled coated liposome.

provides protection against desorption. A retarded drug release in SGF (pH 1.2) when compared to SIF (pH 6.8) was observed as pancreatic enzymes present in SIF disrupt the liposomal membrane, releasing more entrapped ingredients. For an oral delivery system, slow release of the drug in SGF is desirable for more drugs to be available for absorption in the intestine. Overall, a controlled and prolonged drug release was observed for CS-EXE-GEN-LIPO, showing the potential for long-term accessibility of the drug in physiological fluids. Moreover, for efficient tumor growth inhibition *in vivo*, less than 50% drug release in 2 h is acceptable.

Additionally, release patterns were fitted to various kinetic models; based on the correlation coefficient, the best-fit model was chosen, and it was observed that based on the highest R^2 value when compared to different diffusion models, CS-EXE-GEN-LIPO followed Korsmeyer-Peppas model and the n values of 0.19 and 0.1 for EXE and GEN, respectively, follow Fickian diffusion as demonstrated in Figure S1i,ii.

3.5. Animal Studies. *3.5.1. Ex Vivo.* The permeabilities of EXE and GEN from the optimized CS-EXE-GEN-LIPO and from EXE-GEN-SUSP, EXE-SUSP, GEN-SUSP, and EXE-GEN-LIPO were determined by intestinal permeation study using the gut sac method. As demonstrated in Figure 8,

https://doi.org/10.1021/acsomega.3c09948
ACS Omega 2024, 9, 9735−9752

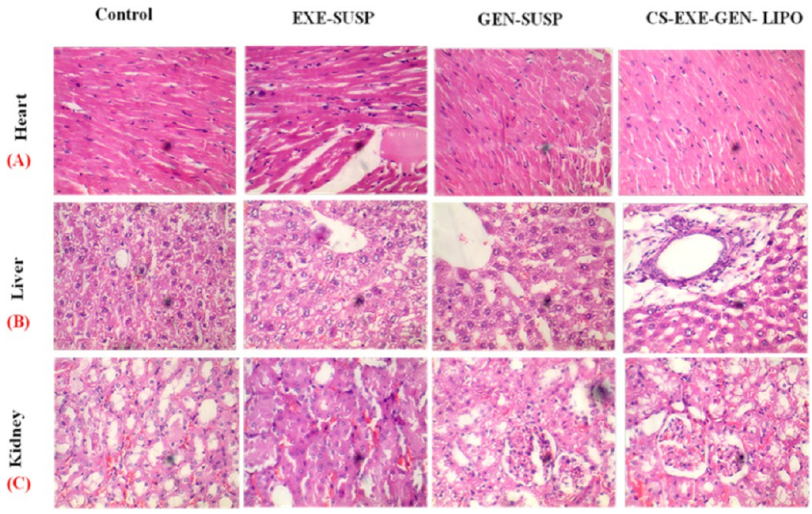

Figure 10. Histopathological photomicrographs of (A) heart, (B) liver, and (C) kidney of female Wistar rats treated with control, EXE-SUSP, GEN-SUSP, and CS-EXE-GEN-LIPO (40x).

optimized CS-EXE-GEN-LIPO when compared to EXE-GEN-LIPO showed a higher cumulative amount of drug permeated with respect to time. In comparison with EXE-SUSP, GEN-SUSP, EXE-GEN-SUSP and EXE-GEN-LIPO, an elevated amount of EXE and GEN was found to be transported from CS-EXE-GEN-LIPO through the membrane by plotting the cumulative amount of drug transported ($\mu g/cm^2$) with respect to time, and subsequently flux was calculated. The apparent permeability coefficient (P_{app}) for EXE and GEN from CS-EXE-GEN-LIPO, EXE-GEN-LIPO, EXE-GEN-SUSP, EXE-SUSP, and GEN-SUSP was found to be 3.88×10^{-4}, 4.27×10^{-4}, 2.98×10^{-4}, 3.12×10^{-4}, 1.56×10^{-4}, 2.10×10^{-4}, 0.35×10^{-4}, and 0.79×10^{-4} cm/min, respectively. Owing to the successful inclusion of EXE and GEN in liposomes facilitating dissolution along with enhanced intestinal permeation of the drug, higher P_{app} values for EXE and GEN were observed for CS-EXE-GEN-LIPO and EXE-GEN-LIPO in comparison with EXE-GEN-SUSP, EXE-SUSP, and GEN-SUSP. The presence of surfactants, cholesterol, and lipids in the liposome formulation is the reason for the higher permeation of liposomes by solubility enhancement of the poorly soluble drug and by reducing the barrier property at the site of absorption when compared with the individual drug suspension. However, in CS-EXE-GEN-LIPO, the positive charge of chitosan due to the amino group interrelates with the negative charge of the intestinal membrane, thereby providing advanced permeation across the mucosal surface by disordering the rigid junction in the mucosa. Another possible explanation for the enhanced permeation of CS-EXE-GEN-LIPO in comparison with EXE-GEN-LIPO is that encapsulation of drugs in the chitosan-coated liposomes makes it unavailable for the P-gp pump and therefore, it can be easily transported across the intestinal wall for absorption.[25]

3.5.2. Confocal Laser Scanning Microscopy (CLSM) Study. CS-EXE-GEN-LIPO was evaluated for its improved permeation in comparison to EXE-GEN-LIPO by confocal microscopy, and the penetration intensity of the dye within the layers of intestinal lumen was analyzed. As depicted in Figure 9, the depth of penetration was calculated at 25 μm for rhodamine B suspension, rhodamine B-labeled uncoated liposomes, and rhodamine B-labeled coated liposomes through the fluorescent images obtained along the *z*-axis. The less fluorescence intensity of the CLSM images of rhodamine B was exhibited merely up to 15 μm, implying that only a few exterior layers were penetrated. However, rhodamine B-labeled uncoated liposomes exhibited fluorescence intensity up to 20 μm. Conversely, in the rhodamine B-loaded CS, the LIPO fluorescence intensity was amplified up to 25 μm, leading to elevated penetration due to the nano size of liposomes and additionally due to the chitosan coating used in the formulation process. A similar observation of elevated permeation was reported in a previous study by Fakhria et al.[34,35]

3.5.3. Toxicity Studies. After oral administration of EXE-SUSP, GEN-SUSP, and CS-EXE-GEN-LIPO, the vital organs, specifically liver, kidney, and heart, were separated, and histopathological studies were performed as shown in Figure 10. Throughout the study period, no considerable changes in weight were observed in the treated groups.

Treatment groups with GEN-SUSP and CS-EXE-GEN-LIPO showed normal histopathology in the cross section of the heart as depicted in Figure 10A. A sustained polarity and well-organized myocytes were observed with no necrosis. Nonetheless, for the EXE-SUSP-treated group, enlarged blood vessels and an inflammatory cell infiltrate with loss of intercalated disc and hemorrhage were noticeable in the segment of the heart.

Furthermore, in a cross section of the liver treated with EXE-SUSP as shown in Figure 10B, exemplified placid toxicity with vacuolated hepatocytes was observed. Groups treated with GEN-SUSP and CS-EXE-GEN-LIPO showed the customary architecture of hepatocytes.

Moreover, the EXE-SUSP-treated group in the cross section of the kidney portrayed trivial disorganization besides relapse and internal bleeding. However, groups treated with GEN-SUSP and CS-EXE-GEN-LIPO showed the presence of medulla, glomeruli, and proximal and distal convoluted tubules in the entire cross section of the kidney. Loops of henle and interstitium were also discernible in all of the treatment groups as depicted in Figure 10C.

In view of the fact that on their monotonous application, no toxicity was observed, it was presumed that the developed CS-EXE-GEN-LIPO was safe and biocompatible for oral administration as there was lack of any noteworthy discrepancy

https://doi.org/10.1021/acsomega.3c09948
ACS Omega 2024, 9, 9735−9752

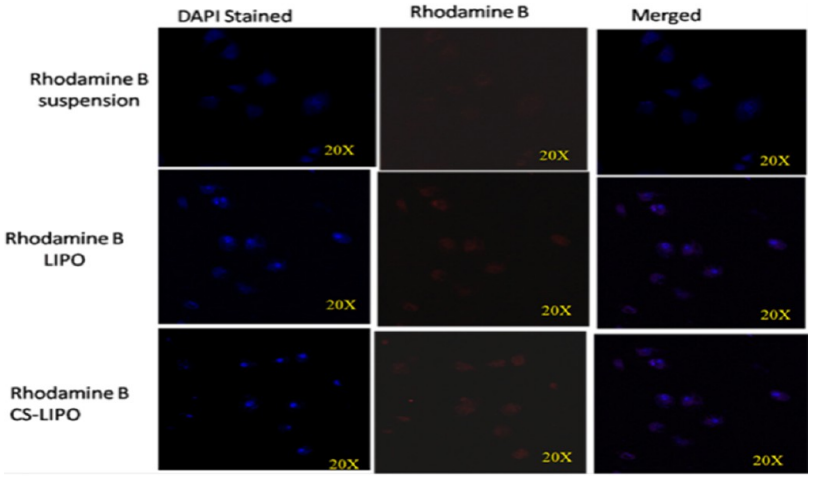

Figure 11. Cellular uptake study performed on MCF-7 cells for plain Rhodamine B solution, Rhodamine B uncoated LIPO, and Rhodamine B Chitosan LIPO at 20×.

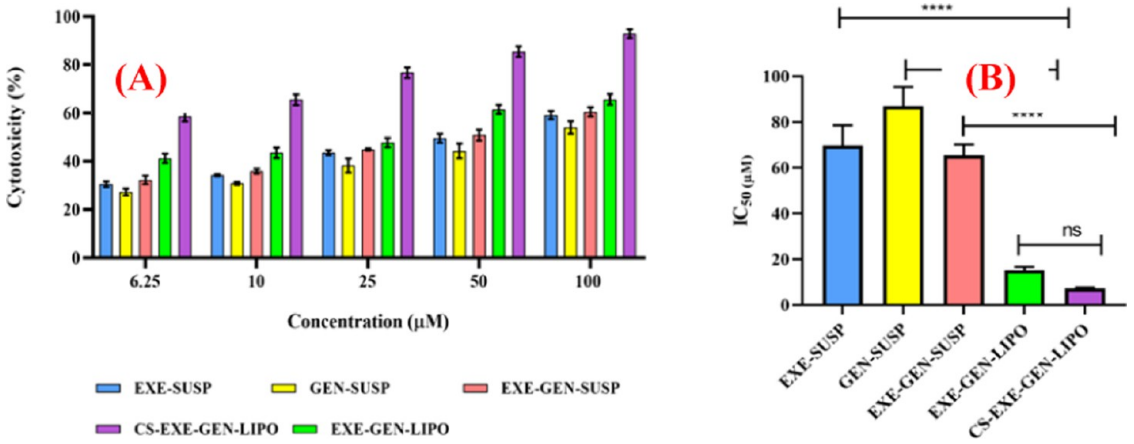

Figure 12. (A) Cell cytotoxicity (%) of MCF-7 cells treated with EXE-SUSP, GEN-SUSP, EXE-GEN-SUSP, EXE-GEN-LIPO, and CS-EXE-GEN-LIPO. (B) IC_{50} values obtained for EXE-SUSP, GEN-SUSP, EXE-GEN-SUSP, EXE-GEN-LIPO, and CS-EXE-GEN-LIPO. The results are expressed as percentage mean ± SD (n = 3) and *p < 0.05, **p < 0.01, ***p < 0.001 and ****p < 0.0001.

among the histological sections of the heart, liver, and kidney treated with altered groups. In conclusion, it was observed that the toxicity related to EXE when administered alone was more when compared to coadministration of EXE with GEN, signifying its probable defensive prospective of GEN.

3.6. Cell Line Studies. *3.6.1. Cellular Uptake Study.* Rhodamine B CS-LIPO and plain Rhodamine B solutions were analyzed for their cellular uptake capability. The red fluorescence as depicted in Figure 11 demonstrates a higher uptake of Rhodamine B CS-LIPO in cells, indicating augmented penetration of the liposomes mainly in the cytoplasm region and more intensely in the nucleus owing to positively charged chitosan coating that could uphold endocytic cellular uptake via cell membrane interaction and the small size of liposomes lying in the nanometric range resulting in immense incorporation inside the cells.[36] The higher uptake displayed by rhodamine B-loaded CS-LIPO is anticipated to result in a more efficient antitumor action. However, plain rhodamine B dye in the rhodamine B solution cell was incapable of penetrating the MCF-7 cells.

3.6.2. In Vitro Cytotoxicity Studies of MTT. The *in vitro* cytotoxicities of EXE-SUSP, GEN-SUSP, EXE-GEN-SUSP, placebo LIPO, EXE-GEN-LIPO, and CS-EXE-GEN-LIPO were assessed by MTT assay at different concentrations (6.25, 10, 25, 50, and 100 μg/mL) on MCF-7 cells as illustrated in Figure 12. CS-EXE-GEN-LIPO exhibited the highest % cytotoxicity in a dose-dependent manner owing to the coencapsulation of EXE with GEN, which chemosensitized the breast cancer cells. The improved cellular uptake of chitosan-coated liposomes inside the cancerous cells as conferred in the above-mentioned studies due to their surface modification and the sustained release of drugs from coated liposomes for a prolonged period providing effective killing of the cells are probable reasons for the enhanced % cytotoxicity.[37]

The placebo LIPO portrayed no toxicity (data not illustrated), while the % cell cytotoxicities of EXE-SUSP (IC_{50}: 69.68 μM ± 8.90 μM), GEN-SUSP (IC_{50}: 86.992 ± 8.376 μM), EXE-GEN-SUSP (IC_{50}: 65.14 ± 1.62 μM), EXE-GEN-LIPO (IC_{50}: 15.18 ± 1.52 μM), and CS-EXE-GEN-LIPO (IC_{50}: 7.253 ± 0.34 μM) are illustrated in Figure 12B.

From the consequences of the current study, it is apparent that in comparison to the individual drugs and combinatorial liposomes, chitosan-coated liposomes demonstrated enhanced cell cytotoxic effects toward MCF-7 cells and consequently can be examined further for successful breast cancer management.

https://doi.org/10.1021/acsomega.3c09948
ACS Omega 2024, 9, 9735−9752

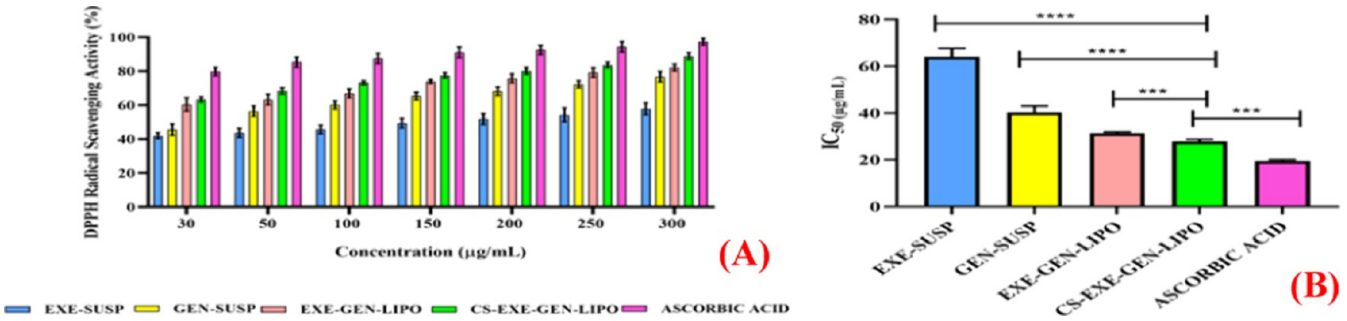

Figure 13. (A) Antioxidant activity of EXE-SUSP, GEN-SUSP, EXE-GEN-LIPO, CS-EXE-GEN-LIPO, and ascorbic acid as estimated by DPPH assay. (B) IC_{50} values obtained for EXE-SUSP, GEN-SUSP, EXE-GEN-LIPO, CS-EXE-GEN-LIPO, and ascorbic acid. The results are expressed as percentage mean ± SD (n = 3) and ***p < 0.001, ****p < 0.0001.

Table 3. Stability Studies Performed on Optimized Lyophilized EXE-GEN-LIPO and CS-EXE-GEN-LIPO at Different Time Durations[a]

			entrapment efficiency (%)	
time (months)	particle size (nm)	PDI	EXE	GEN
		Uncoated Liposomes		
0	104.6 ± 3.8	0.399 ± 0.03	76.8 ± 2.9	74.56 ± 2.1
1	106.44 ± 4.1	0.410 ± 0.04	73.99 ± 1.9	70.12 ± 2.9
3	130.77 ± 2.5	0.439 ± 0.08	70.89 ± 2.4	67.99 ± 2.4
6	160.3 ± 3.2	0.480 ± 0.05	65.80 ± 3.2	62.99 ± 1.9
		Coated Liposomes		
0	120.3 ± 6.40	0.381 ± 0.05	77.5 ± 3.30	76.5 ± 3.20
1	121.4 ± 5.20	0.389 ± 0.03	75.3 ± 3.12	75.7 ± 3.18
3	123.6 ± 3.32	0.399 ± 0.02	73.8 ± 2.67	73.3 ± 2.57
6	125.9 ± 7.12	0.450 ± 0.01	70.6 ± 1.50	71.5 ± 2.10

[a]Results are expressed as the mean ± SD, n = 3.

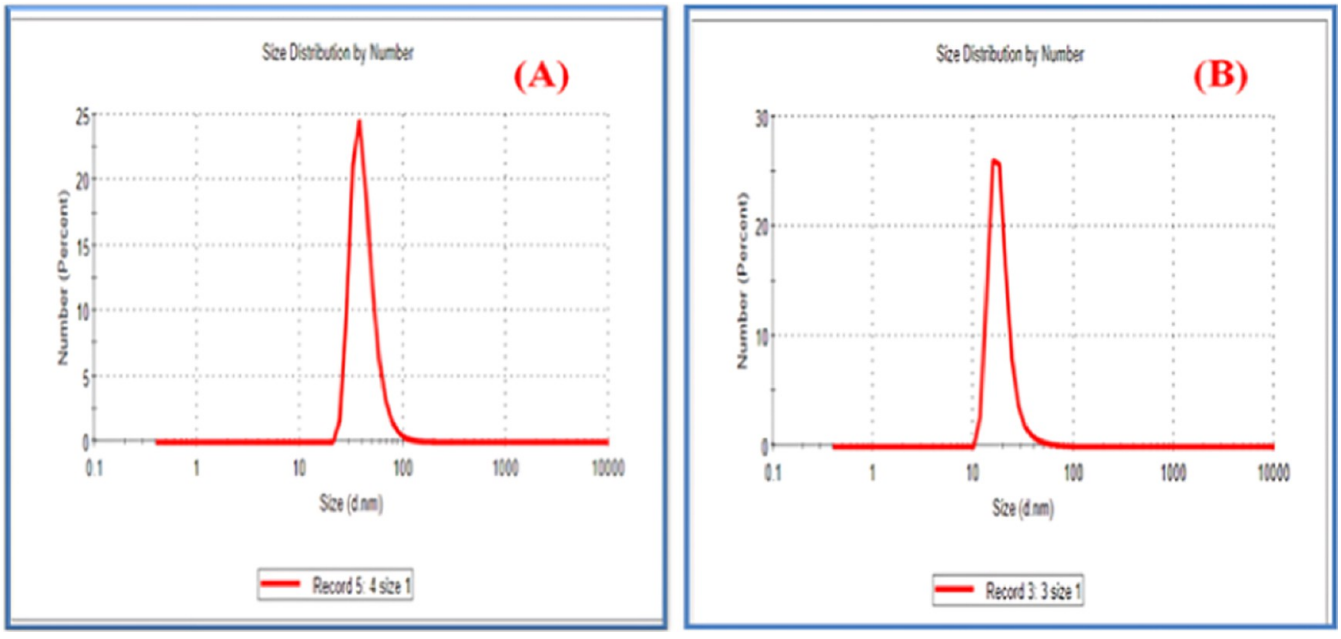

Figure 14. Particle size of (A) uncoated liposomes and (B) coated liposomes after 6 months of storage.

3.6.3. DPPH Radical Scavenging Ability. At different concentrations, free radical scavenging activities of EXE-SUSP, GEN-SUSP, EXE-GEN-LIPO, and CS-EXE-GEN-LIPO were determined. For radical scavenging activity, ascorbic acid was taken as a standard and the DPPH radical assay is illustrated in Figure 13. The radical scavenging activity was found to be 57.99, 76.99, 82.11, 94.56, and 97.67% for EXE-SUSP, GEN-SUSP, EXE-GEN-LIPO, CS-EXE-GEN-LIPO, and ascorbic acid, respectively. Owing to the coating of chitosan, CS-EXE-GEN-LIPO showed a slightly increased antioxidant activity when compared to EXE-GEN-LIPO due to the formation of new H bonds or improvement of existing H

https://doi.org/10.1021/acsomega.3c09948
ACS Omega 2024, 9, 9735−9752

bonds during the encapsulation process.[38] Additionally, EXE-SUSP, GEN-SUSP, EXE-GEN-LIPO, CS-EXE-GEN-LIPO, and ascorbic acid exhibited IC_{50} values of 64.1 ± 3.6, 40.4 ± 2.6, 31.2 ± 0.6, 27.9 ± 0.9, and 19.5 ± 0.5 μg/mL, respectively.

3.7. Storage Stability Study. Aggregation of vesicles and drug leakage result in physical instability. The particle size, PDI, and % EE of freshly prepared lyophilized EXE-GEN-LIPO and CS-EXE-GEN-LIPO were studied for six months. As displayed in Table 3, the mean particle size of EXE-GEN-LIPO increased significantly, whereas CS-EXE-GEN-LIPO did not show remarkable changes, suggesting the good storage stability of the prepared chitosan-coated liposomes. CS-EXE-GEN-LIPO protects the structure of the phospholipid bilayer membrane, thus avoiding leakage and providing enhanced stability.[39] Figure 14 illustrates the particle size of uncoated and coated liposomes after six months of storage period.

4. CONCLUSIONS

In precedent times, oral drug delivery systems in cancer management were difficult to envisage, although the use of oral delivery of anticancer drugs is escalating at the present time. Numerous rational advancements intended to develop or redevelop chemotherapeutic drugs using lipid-based nanotechnology have been accessed by unlocking the budding perceptive of the GI barrier. An imperative aspect to be investigated was the stability issue of orally administered liposomes as the vesicles cannot endure the harsh conditions of the GIT and get degraded quickly without reaching the action site. Surface adornment by chitosan imparts superior drug loading capacity, stability, and protection from GIT, assuring extended release time of the drug, thereby facilitating the drug's reaching the action site and, at the end, augmenting the absorption and bioavailability of the drug. In the present research work, chitosan-coated lipid-based carrier systems coencapsulating exemestane and genistein with therapeutic efficacy in the treatment of breast cancer were successfully developed and investigated. The remarkable advancements in the biopharmaceutical performance of the drug have been interpreted by characterization studies of the prepared chitosan-coated formulation along with individual suspensions of EXE and GEN and EXE-GEN-LIPO (uncoated). Uncoated liposomes and coated liposomes demonstrated particle sizes of 104.6 ± 3.8 nm with a PDI of 0.551 nm and 120.3 ± 6.4 nm with a PDI of 0.381, respectively. The encapsulation efficiency of EXE and GEN in CS-EXE-GEN-LIPO was found to be increased compared to uncoated liposomes. Furthermore, the antioxidant activity and % cell cytotoxicity on MCF-7 cell lines were studied; significant antioxidant activity and enhanced cytotoxicity were displayed by the coated liposomes when compared with the individual drug suspension and uncoated liposomes. The *ex vivo* gut permeation and acute toxicity were studied and, on the basis of the results achieved in the present study, it can be concluded that the developed EXE and GEN-coated liposome could act as a capable drug delivery system for combating breast cancer.

■ ASSOCIATED CONTENT

Supporting Information

The Supporting Information is available free of charge at https://pubs.acs.org/doi/10.1021/acsomega.3c09948.

In vitro kinetic model of EXE and GEN (PDF)

■ AUTHOR INFORMATION

Corresponding Authors

Divya Vohora − *Department of Pharmacology, School of Pharmaceutical Education and Research, Jamia Hamdard, New Delhi 110062, India*; Email: dvohora@jamiahamdard.ac.in

Kanchan Kohli − *Department of Pharmaceutics, School of Pharmaceutical Education & Research, Jamia Hamdard, New Delhi 110062, India; Lloyd Institute of Management & Technology (Pharm.), Greater Noida 201308 Uttar Pradesh, India*; orcid.org/0000-0003-4635-2821; Email: kanchankohli50@gmail.com

Authors

Shwetakshi Sharma − *Department of Pharmaceutics, School of Pharmaceutical Education & Research, Jamia Hamdard, New Delhi 110062, India*; orcid.org/0000-0001-8881-4276

Priya Gupta − *Department of Pharmaceutics, School of Pharmaceutical Education & Research, Jamia Hamdard, New Delhi 110062, India; Lloyd School of Pharmacy, Greater Noida 201306, India*; orcid.org/0000-0002-9296-5904

S. M. Kawish − *Department of Pharmaceutics, School of Pharmaceutical Education & Research, Jamia Hamdard, New Delhi 110062, India*

Shahnawaz Ahmad − *Department of Pharmacology, School of Pharmaceutical Education and Research, Jamia Hamdard, New Delhi 110062, India*

Zeenat Iqbal − *Department of Pharmaceutics, School of Pharmaceutical Education & Research, Jamia Hamdard, New Delhi 110062, India*; orcid.org/0000-0003-2788-9420

Complete contact information is available at: https://pubs.acs.org/10.1021/acsomega.3c09948

Author Contributions

S.S.: Conceptualization, methodology, data curation and writing—original draft. P.G.: Formal analysis, review, and editing. S.M.K.: Writing—review and editing. S.A.: Resources and formal analysis. Z.I.: Project administration. K.K.: Supervision, conceptualization, and project administration. D.V.: Conceptualization and project administration.

Funding

The author (S.S.) would like to recognize the Indian Council of Medical Research (ICMR) for granting fellowship to S.S. (fellowship ID 45/36/2020-Nan/BMS).

Notes

The authors declare no competing financial interest.

■ ACKNOWLEDGMENTS

The authors are thankful to DST-FIST for providing financial assistance to the Department of Pharmaceutics, SPER, Jamia Hamdard. We would like to also acknowledge Jamia Hamdard, New Delhi, India for providing the research facility.

■ REFERENCES

(1) Arnold, M.; Morgan, E.; Rumgay, H.; Mafra, A.; Singh, D.; Laversanne, M.; Vignat, J.; Gralow, J. R.; Cardoso, F.; Siesling, S.; Soerjomataram, I. Current and Future Burden of Breast Cancer: Global Statistics for 2020 and 2040. *Breast* **2022**, *66*, 15−23.

(2) Sung, H.; Ferlay, J.; Siegel, R. L.; Laversanne, M.; Soerjomataram, I.; Jemal, A.; Bray, F. Global Cancer Statistics 2020: GLOBOCAN Estimates of Incidence and Mortality Worldwide for 36 Cancers in 185 Countries. *Ca-Cancer J. Clin.* **2021**, *71* (3), 209−249.
(3) Anderson, B. O.; Ilbawi, A. M.; Fidarova, E.; Weiderpass, E.; Stevens, L.; Abdel-Wahab, M.; Mikkelsen, B. The Global Breast Cancer Initiative: A Strategic Collaboration to Strengthen Health Care for Non-Communicable Diseases. *Lancet Oncol.* **2021**, *22* (5), 578−581.
(4) Kawish, S. M.; Hasan, N.; Beg, S.; Qadir, A.; Jain, G. K.; Aqil, M.; Ahmad, F. J. Docetaxel-Loaded Borage Seed Oil Nanoemulsion with Improved Antitumor Activity for Solid Tumor Treatment: Formulation Development, in Vitro, in Silico and in Vivo Evaluation. *J. Drug Delivery Sci. Technol.* **2022**, *75*, No. 103693.
(5) Meng, J.; Guo, F.; Xu, H.; Liang, W.; Wang, C.; Yang, X.-D. Combination Therapy Using Co-Encapsulated Resveratrol and Paclitaxel in Liposomes for Drug Resistance Reversal in Breast Cancer Cells in Vivo. *Sci. Rep.* **2016**, *6*, No. 22390.
(6) Rizwanullah, M.; Perwez, A.; Mir, S. R.; Alam Rizvi, M. M.; Amin, S. Exemestane Encapsulated Polymer-Lipid Hybrid Nanoparticles for Improved Efficacy against Breast Cancer: Optimization, in Vitrocharacterization and Cell Culture Studies. *Nanotechnology* **2021**, *32* (41), No. 415101.
(7) Chodon, D.; Ramamurty, N.; Sakthisekaran, D. Preliminary Studies on Induction of Apoptosis by Genistein on HepG2 Cell Line. *Toxicol. In Vitro* **2007**, *21* (5), 887−891.
(8) Gossner, G.; Choi, M.; Tan, L.; Fogoros, S.; Griffith, K. A.; Kuenker, M.; Liu, J. R. Genistein-Induced Apoptosis and Autophagocytosis in Ovarian Cancer Cells. *Gynecol. Oncol.* **2007**, *105* (1), 23−30.
(9) Raffoul, J. J.; Wang, Y.; Kucuk, O.; Forman, J. D.; Sarkar, F. H.; Hillman, G. G. Genistein Inhibits Radiation-Induced Activation of NF-KB in Prostate Cancer Cells Promoting Apoptosis and G2/M Cell Cycle Arrest. *BMC Cancer* **2006**, *6* (1), 107.
(10) Choi, E. J.; Lee, B. H. Evidence for Genistein Mediated Cytotoxicity and Apoptosis in Rat Brain. *Life Sci.* **2004**, *75* (4), 499−509.
(11) Atlante, A.; Bobba, A.; Paventi, G.; Pizzuto, R.; Passarella, S. Genistein and Daidzein Prevent Low Potassium-Dependent Apoptosis of Cerebellar Granule Cells. *Biochem. Pharmacol.* **2010**, *79* (5), 758−767.
(12) Banerjee, S.; Li, Y.; Wang, Z.; Sarkar, F. H. Multi-Targeted Therapy of Cancer by Genistein. *Cancer Lett.* **2008**, *269* (2), 226−242.
(13) Sakla, M. S.; Shenouda, N. S.; Ansell, P. J.; Macdonald, R. S.; Lubahn, D. B. Genistein Affects HER2 Protein Concentration, Activation, and Promoter Regulation in BT-474 Human Breast Cancer Cells. *Endocrine* **2007**, *32* (1), 69−78.
(14) Hu, C.-M. J.; Aryal, S.; Zhang, L. Nanoparticle-Assisted Combination Therapies for Effective Cancer Treatment. *Ther. Delivery* **2010**, *1* (2), 323−334.
(15) Alavi, M.; Karimi, N.; Safaei, M. Application of Various Types of Liposomes in Drug Delivery Systems. *Adv. Pharm. Bull.* **2017**, *7* (1), 3−9.
(16) Taléns-Visconti, R.; Díez-Sales, O.; de Julián-Ortiz, J. V.; Nácher, A. Nanoliposomes in Cancer Therapy: Marketed Products and Current Clinical Trials. *Int. J. Mol. Sci.* **2022**, *23* (8), No. 4249.
(17) Jain, A.; Jain, S. K. In Vitro Release Kinetics Model Fitting of Liposomes: An Insight. *Chem. Phys. Lipids* **2016**, *201*, 28−40.
(18) Sharma, S.; Gupta, P.; Gupta, A.; Kawish, S. M.; Iqbal, Z.; Vohora, D.; Kohli, K. Rapid Analytical Method Development and Validation of RP-HPLC Method for the Simultaneous Estimation of Exemestane and Genistein with Specific Application in Lipid-Based Nanoformulations. *ACS Omega* **2023**, *8*, No. 25101.
(19) Bian, Y.; Gao, D.; Liu, Y.; Li, N.; Zhang, X.; Zheng, R. Y.; Wang, Q.; Luo, L.; Dai, K. Preparation and Study on Anti-Tumor Effect of Chitosan-Coated Oleanolic Acid Liposomes. *RSC Adv.* **2015**, *5* (24), 18725−18732.
(20) Cuomo, F.; Cofelice, M.; Venditti, F.; Ceglie, A.; Miguel, M.; Lindman, B.; Lopez, F. In-Vitro Digestion of Curcumin Loaded Chitosan-Coated Liposomes. *Colloids Surf., B* **2018**, *168*, 29−34.
(21) Ezzat, H. M.; Elnaggar, Y. S. R.; Abdallah, O. Y. Improved Oral Bioavailability of the Anticancer Drug Catechin Using Chitosomes: Design, in-Vitro Appraisal and in-Vivo Studies. *Int. J. Pharm.* **2019**, *565*, 488−498.
(22) Khalil, M.; Hashmi, U.; Riaz, R.; Rukh Abbas, S. Chitosan Coated Liposomes (CCL) Containing Triamcinolone Acetonide for Sustained Delivery: A Potential Topical Treatment for Posterior Segment Diseases. *Int. J. Biol. Macromol.* **2020**, *143*, 483−491.
(23) Wu, Z. H.; Ping, Q. N.; Wei, Y.; Lai, J. M. Hypoglycemic Efficacy of Chitosan-Coated Insulin Liposomes after Oral Administration in Mice. *Acta Pharmacol. Sin.* **2004**, *25* (7), 966−972.
(24) Kang, X. J.; Wang, H. Y.; Peng, H. G.; Chen, B. F.; Zhang, W. Y.; Wu, A. H.; Xu, Q.; Huang, Y. Z. Codelivery of Dihydroartemisinin and Doxorubicin in Mannosylated Liposomes for Drug-Resistant Colon Cancer Therapy. *Acta Pharmacol. Sin.* **2017**, *38* (6), 885−896.
(25) Imam, S. S.; Alshehri, S.; Altamimi, M. A.; Hussain, A.; Qamar, W.; Gilani, S. J.; Zafar, A.; Alruwaili, N. K.; Alanazi, S.; Almutairy, B. K. Formulation of Piperine-Chitosan-Coated Liposomes: Characterization and in Vitro Cytotoxic Evaluation. *Molecules* **2021**, *26* (11), 1−13.
(26) Lee, E. H.; Lim, S. J.; Lee, M. K. Chitosan-Coated Liposomes to Stabilize and Enhance Transdermal Delivery of Indocyanine Green for Photodynamic Therapy of Melanoma. *Carbohydr. Polym.* **2019**, *224*, No. 115143.
(27) Ran, L.; Chi, Y.; Huang, Y.; He, Q.; Ren, Y. Synergistic Antioxidant Effect of Glutathione and Edible Phenolic Acids and Improvement of the Activity Protection by Coencapsulation into Chitosan-Coated Liposomes. *LWT–Food Sci. Technol.* **2020**, *127* (24), No. 109409.
(28) Nguyen, T. X.; Huang, L.; Liu, L.; Elamin Abdalla, A. M.; Gauthier, M.; Yang, G. Chitosan-Coated Nano-Liposomes for the Oral Delivery of Berberine Hydrochloride. *J. Mater. Chem. B* **2014**, *2* (41), 7149−7159.
(29) Singh, A.; Neupane, Y. R.; Mangla, B.; Kohli, K. Nanostructured Lipid Carriers for Oral Bioavailability Enhancement of Exemestane: Formulation Design, In Vitro, Ex Vivo, and In Vivo Studies. *J. Pharm. Sci.* **2019**, *108* (10), 3382−3395.
(30) Mangla, B.; Neupane, Y. R.; Singh, A.; Kumar, P.; Shafi, S.; Kohli, K. Lipid-Nanopotentiated Combinatorial Delivery of Tamoxifen and Sulforaphane: Ex Vivo, in Vivo and Toxicity Studies. *Nanomedicine* **2020**, *15* (26), 2563−2583.
(31) Mazloomi, S. N.; Mahoonak, A. S.; Ghorbani, M.; Houshmand, G. Physicochemical Properties of Chitosan-Coated Nanoliposome Loaded with Orange Seed Protein Hydrolysate. *J. Food Eng.* **2020**, *280*, No. 109976.
(32) Kozhikhova, K. V.; Ivantsova, M. N.; Tokareva, M. I.; Shulepov, I. D.; Tretiyakov, A. V.; Shaidarov, L. V.; Rusinov, V. L.; Mironov, M. A. Preparation of Chitosan-Coated Liposomes as a Novel Carrier System for the Antiviral Drug Triazavirin. *Pharm. Dev. Technol.* **2018**, *23* (4), 334−342.
(33) Gu, Y.; Zhao, Z.; Xue, F.; Zhang, Y. Alginate-Chitosan Coated Nanoliposomes as Effective Delivery Systems for Bamboo Leaf Flavonoids: Characterization, In Vitro Release, Skin Permeation and Anti-Senescence Activity. *Antioxidants* **2022**, *11* (5), No. 1024.
(34) Fakhria, A.; Sarim, S.; et al. Formulation of Thymoquinone Loaded Chitosan Nano Vesicles: In-Vitro Evaluation and in-Vivo Anti-Hyperlipidemic Assessment. *J. Drug Delivery Sci. Technol.* **2019**, *50*, 339−346.
(35) Shin, G. H.; Chung, S. K.; Kim, J. T.; Joung, H. J.; Park, H. J. Preparation of Chitosan-Coated Nanoliposomes for Improving the Mucoadhesive Property of Curcumin Using the Ethanol Injection Method. *J. Agric. Food Chem.* **2013**, *61* (46), 11119−11126.
(36) Aboumanei, M. H.; Mahmoud, A. F.; Motaleb, M. A. Formulation of Chitosan Coated Nanoliposomes for the Oral Delivery of Colistin Sulfate: In Vitro Characterization, 99mTc-

https://doi.org/10.1021/acsomega.3c09948
ACS Omega 2024, 9, 9735−9752

Radiolabeling and in Vivo Biodistribution Studies. *Drug Dev. Ind. Pharm.* **2021**, *47* (4), 626−635.
(37) Xiao, Y.; Ho, C. T.; Chen, Y.; Wang, Y.; Wei, Z.; Dong, M.; Huang, Q. Synthesis, Characterization, and Evaluation of Genistein-Loaded Zein/Carboxymethyl Chitosan Nanoparticles with Improved Water Dispersibility, Enhanced Antioxidant Activity, and Controlled Release Property. *Foods* **2020**, *9* (11), No. 1604.
(38) Seyedabadi, M. M.; Rostami, H.; Jafari, S. M.; Fathi, M. Development and Characterization of Chitosan-Coated Nano-liposomes for Encapsulation of Caffeine. *Food Biosci.* **2021**, *40*, No. 100857.
(39) He, H.; Lu, Y.; Qi, J.; Zhu, Q.; Chen, Z.; Wu, W. Adapting Liposomes for Oral Drug Delivery. *Acta Pharm. Sin. B* **2019**, *9* (1), 36−48.

https://doi.org/10.1021/acsomega.3c09948
ACS Omega 2024, 9, 9735−9752